AGU ADVANCING EARTH AND SPACE SCIENCE

Water Resources Research

RESEARCH ARTICLE
10.1029/2020WR028390

Sequential Data Assimilation for Streamflow Forecasting: Assessing the Sensitivity to Uncertainties and Updated Variables of a Conceptual Hydrological Model at Basin Scale

G. Piazzi[1], G. Thirel[1], C. Perrin[1], and O. Delaigue[1]

[1]Université Paris-Saclay, INRAE, UR HYCAR, Antony Cedex, France

Key Points:

- Estimation of forecast initial level of the routing store of a conceptual hydrological model ensures the most benefit from data assimilation
- Updating forecast initial conditions using the ensemble Kalman filter results in a greater improvement in predictive accuracy in the short term
- The particle filter guarantees a longer-lasting effect of the update of initial conditions over the forecast horizon

Supporting Information:

Supporting Information may be found in the online version of this article.

Correspondence to:

G. Thirel,
guillaume.thirel@inrae.fr

Citation:

Piazzi, G., Thirel, G., Perrin, C., & Delaigue, O. (2021). Sequential data assimilation for streamflow forecasting: Assessing the sensitivity to uncertainties and updated variables of a conceptual hydrological model at basin scale. *Water Resources Research*, *57*, e2020WR028390. https://doi.org/10.1029/2020WR028390

Received 28 JUL 2020
Accepted 9 JAN 2021

Abstract Skillful streamflow forecasts provide key support to several water-related applications. Because of the critical impact of initial conditions (ICs) on forecast accuracy, ever-growing interest is focused on improving their estimates via data assimilation (DA). This study aims to assess the sensitivity of the DA-based estimation of forecast ICs to several sources of uncertainty and the update of different model states and parameters of a lumped conceptual rainfall–runoff model over 232 watersheds in France. The performance of two sequential ensemble-based techniques, namely, the ensemble Kalman filter (EnKF) and the particle filter (PF), is compared in terms of efficiency and temporal persistence (up to 10 days) of the updating effect through the assimilation of observed discharges. Several experiments specifically address the impact of the meteorological, state, and parameter uncertainties. Results show that an accurate estimate of the initial level of the routing store of the conceptual model ensures the most benefit to the DA-based estimation of forecast ICs. While EnKF-based forecasts outperform PF-based ones when accounting for meteorological uncertainty, the more comprehensive representation of the state uncertainty makes it possible to greatly improve the accuracy of PF-based predictions, with a longer-lasting updating effect. Conversely, forecasting skill is undermined when accounting for parameter uncertainty, owing to the change in hydrological responsiveness. This study extensively addresses several sensitivity analyses in order to provide useful recommendations for designing DA-based streamflow forecasting systems and for diagnosing possible deficiencies in existing systems.

Plain Language Summary Accurate streamflow forecasts are of critical importance to several real-time applications, such as water resource management and flood prevention. The predictive accuracy critically depends on the quality of the forecast initial conditions. Data assimilation (DA) techniques are increasingly being implemented to obtain the most likely estimation of forecast initial conditions through the assimilation of observed hydrological variables. This study compares the performances of two DA techniques, namely the Ensemble Kalman filter and the Particle filter, in terms of both efficiency and temporal persistence (up to 10 days) of the updating effect. The analysis addresses the impact of different sources of uncertainty and the update of different model states and parameters of a lumped conceptual hydrological model, when assimilating observed discharges over 232 watersheds in France. Results show that an accurate estimation of the initial level of the routing store ensures the most benefit of DA, as this state variable is the most correlated with observations. A comprehensive representation of the state uncertainty generally improves the estimation of the forecast initial conditions resulting from the assimilation. While the Ensemble Kalman filter outperforms the Particle filter in the short term, this latter guarantees a longer-lasting updating effect over the forecast horizon.

1. Introduction

In recent decades, the ever-increasing urban sprawl in areas prone to hydrology-related hazard (Szewrański et al., 2018) and the impact of climate change on precipitation patterns (Pfahl et al., 2017) increasingly require efficient management of water resources. Skillful operational streamflow forecasting systems have been developed to support decision-makers in a wide range of real-life applications (Zappa et al., 2018), such as the forecasting of both flooding events (Alfieri & Thielen, 2015; Blöschl et al., 2017) and critical

droughts (Hao et al., 2018; Trambauer et al., 2015), as well as the optimization of hydropower production (Boucher & Ramos, 2018).

The growing awareness of the critical importance of uncertainty in hydrological forecasting is a common issue across most forecasting systems. Blöschl et al. (2019) recently identified the need to untangle and reduce the different sources of uncertainty in model predictions as one of the main unsolved problems in hydrology. Indeed, several sources of uncertainty can jointly affect model simulations, namely, random or systematic errors in model forcings, uncertainty due to suboptimal parameter estimates, and errors due to incomplete or biased model structure (Thiboult et al., 2016). Hence, operational forecasting systems are increasingly turning from single deterministic predictions to probabilistic forecasts, thereby making it possible to take account of most of these uncertainties (Alfieri et al., 2012; Cloke & Pappenberger, 2009). For more than a decade, the international Hydrologic Ensemble Prediction Experiment (HEPEX) initiative has been investigating how best to generate, communicate, and use hydrologic ensemble forecasts (Schaake et al., 2006, 2007).

Several hydrological ensemble forecasting systems are currently operational at regional and national levels and tailored to the spatial and temporal scales of interest, according to the uniqueness of hydrological basins, climate conditions, data availability, and specific end-user demands (Harrigan et al., 2018; Thirel et al., 2008; Werner et al., 2013). Ensemble hydrological forecasting systems are also operational at the continental scale, such as the European Flood Awareness System (EFAS) (Alfieri et al., 2014; Thielen et al., 2009) in Europe, the U.S. Hydrologic Ensemble Forecast Service (HEFS) (Brown et al., 2014), and the African Flood Forecasting System (AFFS) (Thiemig et al., 2015). At even larger scales, the Global Flood Awareness System (GloFAS) (Alfieri et al., 2013) and the Global Flood Forecasting and Information System (GLOFFIS) (Emerton et al., 2016) provide global hydrological forecasts. In recent decades, streamflow predictability has been extended from a few hours to several days or even months, depending on the main forecasting objectives (Cuo et al., 2011).

When dealing with real-time operational applications, a trade-off is necessary between model complexity, data requirements, computational burden, and forecast accuracy (Butts et al., 2004). Even though spatially distributed hydrological models exploit the observed spatial information to provide discharge simulations also at interior points of the watershed, they can be computationally intensive (Young, 2002) and generally sensitive to the calibration strategy (Reed et al., 2004). On the other hand, lumped hydrological models are a reliable operational tool for streamflow forecasting, thanks to their simplicity, computational efficiency, and lower data requirements (Hapuarachchi et al., 2011). Conceptual rainfall–runoff models have proved their effectiveness in streamflow forecasting (e.g., Sacramento model, Burnash et al., 1973; HBV-96 model, Lindström et al., 1997) owing to the small number of parameters to be calibrated. Indeed, an increase in model complexity does not necessarily entail an enhancement in performance, mainly due to limitations in the available calibration data (Reed et al., 2004) and the resulting identifiability problems in parameter estimation (Boyle et al., 2001).

Regardless of the modeling approach, forecast reliability generally decreases throughout the forecast horizon, mainly due to the inherent uncertainty in initial conditions (ICs) and the stochastic behavior of meteorological forcings (Li et al., 2009). Recent works contended that streamflow forecasting skill is mostly controlled by hydrological ICs (Shukla & Lettenmaier, 2011; Wood et al., 2016; Yossef et al., 2013). Hence, ever-growing interest is focused on enhancing forecast ICs by updating model states and/or parameters through the assimilation of available observations into hydrological models to improve forecast accuracy and to quantify predictive uncertainty (Liu et al., 2012). For real-time streamflow forecasting, the assimilation of observed discharges is the most common approach, as this hydrological variable is arguably a key predictor and its measurements are generally readily available (Clark et al., 2008; Ricci et al., 2011; Thirel et al., 2010).

Several data assimilation (DA) techniques, differing in numerical cost and optimality, have been proposed and used to assimilate discharge data into hydrologic models for forecasting purposes (Liu et al., 2012). Sequential DA, also known as filtering, has gained widespread interest in real-time applications, since this approach sequentially updates the system forecasts whenever observations are available (Leisenring & Moradkhani, 2011). Numerous research studies have addressed the potential of sequential DA techniques to

improve the skill of streamflow forecasts through the Kalman filter (KF; Kalman, 1960) (C. H. Wang and Bai, 2008), extended Kalman filter (EKF; Miller et al., 1994) (L. Sun et al., 2015), ensemble Kalman filter (EnKF; Evensen, 1994, 2003) (Blöschl et al., 2008; Rakovec et al., 2012; Samuel et al., 2014; Vrugt et al., 2006; Vrugt & Robinson, 2007), unscented KF (UKF; Julier et al., 1995) (Y. Sun et al., 2020), the particle filter (PF; Arulampalam et al., 2002) (DeChant & Moradkhani, 2014; Yan & Moradkhani, 2016), and variants of the aforementioned filters and smoothers (Noh et al, 2011a, 2013, 2014; Chen et al., 2013; McMillan et al., 2013; Rakovec et al., 2015).

Of the filtering methods, the sequential ensemble-based techniques, such as EnKF and PF, are particularly well-suited to probabilistic streamflow forecasting systems, since their flexible framework makes it possible to explicitly handle different sources of uncertainty and quantify the unknown errors of both model states and observations (Noh et al., 2013). Table A1 in the Appendix A provides a summarized overview of some of the existing studies on this issue, which will be discussed in more detail here.

Thiboult et al. (2016) demonstrated that the EnKF largely contributes to prediction accuracy by reducing and characterizing the uncertainty in ICs, which is identified as the dominant source of uncertainty in streamflow forecasting. However, the effect of the EnKF-based assimilation generally faded out quickly throughout the forecast time window. In order to ensure the improvement of forecast accuracy, Maxwell et al. (2018) pointed out the critical importance of introducing combined mass and flux constraints to preserve the physical consistency of the system when using the EnKF to assimilate observed discharges into a lumped conceptual hydrological model. In the study by DeChant and Moradkhani (2011), the PF revealed an effective potential to improve state initialization of a seasonal streamflow forecasting system when taking account of IC uncertainty in addition to forcing uncertainty. The critical importance of preventing the underestimation of system uncertainty had been stressed by Berthet (2010), who tested the PF scheme within a conceptual hydrological model for streamflow forecasting. Likewise, the PF-based estimation of forecast ICs succeeded in significantly improving seasonal drought probabilistic predictive skill with a sufficiently large lead time (Yan et al., 2017).

Weerts and El Serafy (2006) investigated the suitability of EnKF and PF schemes for operational flood forecasting systems by comparing their performance using a conceptual rainfall–runoff model. While PFs outperform the EnKF for a larger number of particles, the EnKF reveals lower sensitivity to the characterization of system uncertainties and it performs best with a limited ensemble size. More recently, Noh et al. (2013) compared these two ensemble-based sequential DA techniques to assimilate hourly discharge observations into a distributed hydrological model for short-term streamflow forecasting in a small watershed. For different forecast lead times, PF-based forecasts revealed higher and longer-lasting accuracy than the EnKF-based predictions when considering the uncertainty of model states.

Filtering techniques are widely used to estimate dynamic model states, under the assumption of time-invariant parameters, which are usually predefined in advance. However, since there is no guarantee that system behavior does not change over time, a time variation of parameters together with state variables can be an effective approach to improving forecast reliability (Moradkhani, Sorooshian, et al., 2005). Several studies have aimed at assessing the potential of sequential ensemble-based DA techniques in order to simultaneously estimate both model states and parameters. Different EnKF-based approaches have been developed for the joint state–parameter estimate. As an alternative approach to the augmented state vector approach (Reichle et al., 2002; D. Wang et al., 2009; Xie & Zhang, 2010; Young, 2002), Moradkhani, Sorooshian, et al. (2005) presented a dual state–parameter estimation by iteratively using an EnKF scheme in a conceptual rainfall–runoff model for ensemble streamflow forecasting. A further approach was proposed by Xie and Zhang (2013), who assessed an EnKF-based partitioned forecast-update scheme to reduce the degree of freedom of the high-dimensional state space of a distributed hydrologic model. In addition to the EnKF, the PF has been used for joint state–parameter estimation (Guingla et al., 2012; Montzka et al., 2011). Moradkhani, Hsu, et al. (2005) demonstrated the applicability of the PF to jointly assess parameter uncertainty and estimate model states in a conceptual hydrologic model through the assimilation of observed discharges. The usefulness of the PF-based dual state–parameter updating scheme was addressed by Noh et al. (2011b), who demonstrated the resulting higher forecast accuracy compared to updating only the model states of a parsimonious hydrological model.

In most applications, both the EnKF and PF schemes succeed in properly enhancing the accuracy of streamflow forecasts through the assimilation of observed discharges at the time of forecast. Comparative studies detected the main differences between these DA techniques in terms of efficiency (i.e., the PF scheme results in longer-lasting accuracy), sensitivity to the ensemble size (i.e., the EnKF scheme is generally less sensitive), and computational demand. It is noteworthy that several authors pointed out the key importance of accounting for a comprehensive representation of system uncertainties in order to reliably estimate forecast ICs.

Further efforts are needed to extensively investigate the sensitivity of these commonly used DA methods to different uncertainties in hydrological forecasting and how these latter can affect both DA-based predictive accuracy and the temporal persistence of the DA-based ICs, namely how long the benefit of the updating effect lasts over the forecast horizon. Indeed, to the best of the authors' knowledge, no existing study undertakes a comparative analysis of sequential ensemble-based DA schemes in order to thoroughly assess their differences in sensitivity to the main sources of uncertainty and the updating of specific states and parameters of a streamflow forecasting system for operational purposes.

This study aims to assess how and to what extent the DA-based estimation of forecast ICs can effectively improve the predictive accuracy of streamflow forecasts provided by a conceptual rainfall-runoff model. The main objective is to investigate the limits and potentialities of a parsimonious hydrological model when assimilating real-time discharge observations for operational streamflow forecasting purposes. For this purpose, this study specifically addresses the main issues that need to be investigated when designing the optimal configuration of a new forecasting system, as well as when diagnosing possible deficiencies in existing ones. Several experiments were performed to assess the sensitivity of the DA-based estimation of forecast ICs to several sources of uncertainty and to the updating of different model states and parameters. In more detail, the study aims to:

(1) Investigate the performance of two commonly used sequential ensemble-based DA techniques, namely, the EnKF and PF schemes, with the aim of assessing the main differences in terms of both efficiency and the temporal persistence of the ICs updating effect over the forecast horizon
(2) Assess the relative impact of the most relevant uncertainties affecting streamflow forecasts, namely, the uncertainty in meteorological forcings, model parameters, and states, on the accuracy of DA-based estimates of the forecast ICs
(3) Identify the key hydrological processes in a conceptual rainfall–runoff model and thus the most sensitive model states and parameters to be updated in order to achieve the most benefit from the assimilation of observed discharges

Section 2 aims to provide an introduction to sequential ensemble-based DA techniques. After describing the case studies, the datasets, and the hydrological model, Section 3 introduces probabilistic DA-based forecasts, with a focus on the comprehensive representation of system uncertainties. All experiments are then explained in terms of objectives and assumptions, as well as evaluation metrics. The main results are presented in Section 4 and discussed in more detail in Section 5. Finally, conclusions are outlined in Section 6.

2. Sequential Ensemble-Based Data Assimilation

Filtering techniques make it possible to readily process the observational data (Y_t) as they become available and to sequentially update the model state at time t (X_t), which is defined as:

$$X_t = M\left[X_{t-1}, \theta, U_t, \Omega_t\right] \quad (1)$$

where M is the dynamic model operator, which calls for the model input vector (U_t), the vector of the model parameters (θ), and the unknown model error (Ω_t), which is statistically represented by a random stochastic perturbation.

DA integrates observational information to improve prediction accuracy while taking into consideration the uncertainty in both measurements and model predictions. One of the main challenges in DA is estimating the unknown errors affecting both the observations and the model states, which is of critical importance in

order to optimally combine the a priori estimate of the system state (i.e., the background state, X_t^b) with the observations to evaluate the analysis state (X_t^a).

Both EnKF and PF rely on a recursive Bayesian algorithm, based on the key idea of representing each kind of uncertainty through specific probability distributions describing the error statistics. The main difference between the EnKF and the PF is how they recursively generate an approximation to the probability distributions of the prognostic variables by using a set of randomly generated model replicates according to a Monte Carlo approach (Weerts & El Serafy, 2006).

2.1. Ensemble Kalman Filter

The EnKF (Evensen, 1994) provides an analytical solution to the analysis problem by approximating the second-order moments of probability distributions, while assuming Gaussian distributional properties of the prognostic variables. Whenever an observation is available, an analysis procedure is performed through optimal weighting between simulated and observed values, with the degree of correction determined by their degree of uncertainty.

The analysis state of each *i*th ensemble member ($X_{t,i}^a$) is evaluated according to the formula:

$$X_{t,i}^a = X_{t,i}^b + K_t\left[Y_{t,i} - H\left[X_t^b\right]\right] \tag{2}$$

where $X_{t,i}^b$ is the *nstate*-length background state vector of each *i*th ensemble member (*nstate* is the number of state variables), $Y_{t,i}$ is ith *nobs*-length vector of observations (*nobs* is the number of available observations), which are sampled from a distribution with mean equal to the observations at time t and variance R_t (see Section 3.3.5 for further details), H is the *nobs* × *nstate* operator, enabling transition from the model space to the observations space (Evensen, 1994).

The Kalman gain (K_t) is evaluated as a combination of the error covariance matrices of both the model and the observations:

$$K_t = P_t H^T\left(HP_tH^T + R_t\right)^{-1} \tag{3}$$

where R_t is the *nobs* × *nobs* error covariance matrix of observations and P_t is the model error covariance matrix, which is diagnosed from the ensemble and dynamically updated at each assimilation time step (Evensen, 2003).

The definition of the H operator is of critical importance to properly map model states to observations ones. Beside the most conducive application calling for an exact match between observed and modeled quantities, a forward model can be required to derive the model equivalent of the observation from model states. When dealing with a linear forward model, it can be directly included in the H matrix, otherwise the forward model must be run separately.

The EnKF technique also allows for combined state–parameter estimation. One approach is the so-called state augmentation, where parameters are treated as model states and are concatenated with them into a single joint vector (including both θ and X_t) updated by the DA analysis procedure when observations are available (Reichle et al., 2002). Consequently, the covariance matrices are augmented in turn by the covariances between these unknown parameters and each state variable, since model states and parameters are jointly updated (Franssen & Kinzelbach, 2008). However, for high-dimensional systems (e.g., distributed hydrological models), the state augmentation strategy may suffer from spurious over or underestimated correlations between states and parameters, which are likely to directly affect the DA-based parameter estimation (Xie & Zhang, 2013). Moradkhani, Sorooshian, et al. (2005) contended that the increase in the number of unknown variables (i.e., model states and parameters) leads to a greater degree of system freedom, which is likely to make the estimation unstable, especially in highly nonlinear models. An alternative approach to state augmentation is dual estimation, designed as two parallel filters that recursively estimate both model states and parameters (Moradkhani, Sorooshian, et al., 2005). According to dual estimation, the EnKF is

first applied to update the parameters and then reapplied to obtain the analysis states, as a function of the updated parameters.

The major drawback is that the Kalman filtering neglects moments higher than second-order in the analysis step, according to the underlying assumption that both the model states and the observations have a Gaussian distribution (Moradkhani, Hsu, et al., 2005). Indeed, in nonlinear stochastic dynamic systems, the first two moments of the prior density are generally not sufficient to properly approximate the posterior probability distribution, which is unlikely to be Gaussian (Salamon & Feyen, 2009; Weerts & El Serafy, 2006). For such cases, an accurate estimate of posterior probability requires the tracking of higher-order moments (Moradkhani, Hsu, et al., 2005).

2.2. Sequential Importance Resampling Particle Filter

Particle filtering has the main advantage of relaxing the need for a restrictive assumption regarding Gaussian property constraints (Weerts & El Serafy, 2006). Indeed, since the full prior density functions are used within the updating procedure, PF makes it possible to handle the propagation of non-Gaussian distributions through nonlinear models (Arulampalam et al., 2002; Salamon & Feyen, 2009). According to the sequential importance sampling (SIS) approach (Guingla et al., 2012; Moradkhani, Hsu, et al., 2005), the particles are randomly sampled from a known, easy-to-sample proposal distribution to approximate posterior probability. Whenever an observation is available, the importance weights associated with the particles are recursively updated, as a function of the likelihood of particle states with respect to the observed one. Particles are then properly weighted and propagated sequentially by applying Bayes' rule to estimate posterior distribution through an optimal combination of the prior distribution and the likelihood function. However, since the stochastic behavior of the system generally causes dispersion of the particles, only a few particles are likely to have nonzero importance weights after several iterations, while most of them are discarded owing to their negligible probability (Doucet, 1998). This is the well-known sample degeneracy, whereby the particles fail to correctly approximate posterior distribution.

The impact of this undesirable and unavoidable side effect can be mitigated by a resampling procedure, which makes it possible to restore sample variety without affecting characterization of the posterior distribution. Gordon et al. (1993) proposed sequential importance resampling (SIR) to avoid sample degeneracy by introducing a resampling procedure at each time step. The additional resampling step enables to discard particles with a low probability and to replicate those with a high importance weight, while the total number of particles is maintained unchanged. Clearly, particles that are closer to the truth are more likely to be resampled, since the greater the weight of a particle, the higher the number of replications of that particle in the resulting particle set.

When applying the PF for the combined estimate of model states and parameters, the latter are resampled together with the particle states and then perturbed to prevent their sample impoverishment (Moradkhani, Hsu, et al., 2005).

3. Material and Methods

3.1. Watershed Set and Hydrometeorological Data

In order to extensively assess the performance of DA-based streamflow forecasts, this study relies on the large and varied set of 232 watersheds across France set up by Ficchì et al. (2016). According to the classification of the French river flow regimes by Sauquet et al. (2008), the great part of the watersheds is characterized by pluvial river flow regimes. It is noteworthy that snowmelt-fed regimes are not represented in this catchment sample. However, few basins in a pluvio-nival regime are considered in the mountainous areas. Meteorological forcings are derived from the SAFRAN meteorological reanalysis (Vidal et al., 2010), providing both precipitation and temperature data series at the daily time step, which are aggregated at the watershed scale in this lumped application. Potential evapotranspiration is estimated from the SAFRAN temperature according to the temperature-based formulation proposed by Oudin et al. (2005). Daily streamflow data are available at each watershed outlet from the Banque HYDRO database (http://www.hydro.eaufrance.fr; Leleu et al., 2014). In order not to undermine the performance of the forecasting system through

the assimilation of possible unreliable observations, the quality of the measured discharges was investigated through both visual inspection of hydrographs and the quality code on the observation reliability (Delaigue et al., 2020). The analysis period is from January 01, 2006 to December 31, 2011.

3.2. Hydrological Model

GR5J is a daily lumped conceptual model (Le Moine, 2008; Pushpalatha et al., 2011). The rainfall–runoff processes are represented at the watershed scale through an interception function, two main stores, namely, production and routing stores, a unit hydrograph and an exchange function (Figure 1). The production store level (S) accounts for the evolution of the watershed soil moisture content at each time step, depending on both the incoming rainfall to the store (Ps) and the actual evapotranspiration drawn from the store (Es). The routing function relies on a nonlinear routing store (R) and a symmetric unit hydrograph for runoff lagging. The unit hydrograph states (UH) define the streamflow that is routed at each time step. The two runoff components (90% and 10% of effective rainfall Pr, respectively) are estimated. Inflows (outflows) from (to) the outside of the basin are simulated through a groundwater exchange function.

The rainfall–runoff model relies on five free parameters (reported in bold in Figure 1) requiring proper calibration to optimize the accuracy of model simulations: the maximum capacities of both the production and routing stores (X_1 [mm] and X_3 [mm], respectively); a groundwater water exchange coefficient (X_2, [mm/d]) taking either positive (i.e., water inflows) or negative (i.e., water outflows) values; the time base of the unit hydrograph (X_4 [d]); the threshold for groundwater exchange (X_5 [-]). The DA-based streamflow forecasting system was developed using the R package *airGR* (Coron et al., 2017, 2020), providing a constantly up-to-date version of the GR5J model. The snow module was not activated, since no snow-dominated watershed is included in the dataset.

For each watershed, GR5J was calibrated throughout the 6-year analysis period using the Kling–Gupta efficiency (KGE) coefficient (Gupta et al., 2009) as an objective function, evaluated as:

$$KGE = 1 - \sqrt{(r-1)^2 + (a-1)^2 + (b-1)^2} \tag{4}$$

where r is the linear correlation coefficient between simulated and observed streamflow; a is the ratio of the standard deviation of simulated discharges to the standard deviation of observed ones (i.e., an estimate of the relative variability between simulated and observed values); b is the ratio of the mean of simulated discharges to the mean of observed discharges (i.e., a measure of the overall bias). The optimal KGE value is 1. Figure 2 shows the evaluation of the KGE criterion resulting from the calibration procedure over the period 2006–2011. The KGE values reveal good performance of the GR5J model over most of the basins and in different hydrometeorological contexts (KGE values higher than 0.85 for 65% of watersheds).

3.3. Probabilistic DA-Based Forecasts

This study aims to assess the usefulness of estimating forecast ICs to improve the predictive accuracy of forecasts over a horizon of 10 days, in terms of both efficiency and temporal persistence. Therefore, DA-based streamflow forecasts are performed daily starting from the updated ICs resulting from the assimilation of the last available observation at the forecast time step (Figure 3, DA-IC). Thanks to more accurate ICs, DA-based forecasts are supposed to be more reliable than open loop (OL) predictions, which do not rely on the assimilation of observed discharges (Figure 3, OL-IC). It is noteworthy that both DA-based and OL streamflow forecasts are driven by perfect 10-day meteorological forecasts, namely, the posteriori observations of rainfall and potential evapotranspiration. This choice makes it possible to assess the performance of the DA-based forecasting system by preventing any superimposed effect of the unknown errors affecting meteorological forecasts.

3.3.1. Implementation Details of DA Schemes

Both the EnKF and the PF schemes consider the same state vector (X_t), which can encompass the production store level (S), the routing store level (R) and the unit hydrograph state (UH) (Figure 4), depending on the experiments (see Section 3.4 for further details). When dealing with the dual estimation of both

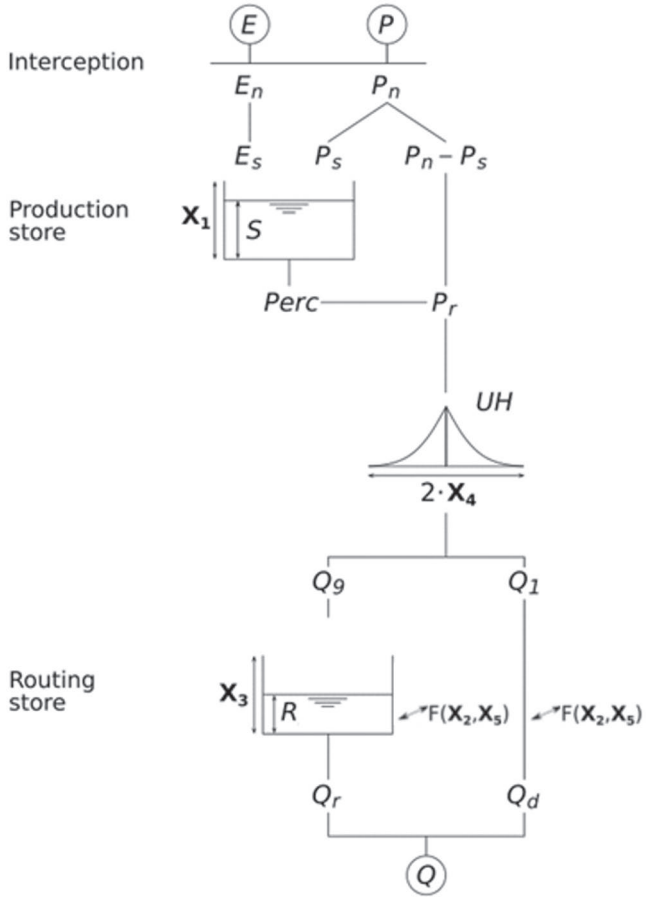

Figure 1. Scheme of the GR5J hydrological model (Le Moine, 2008). *E*, evapotranspiration; *P*, areal basin rainfall; *Pn*, net precipitation; *En*, net evapotranspiration; *S*, production store; *Perc*, percolation amount; *R*, routing store; Q_9 and Q_1, outputs of the unit hydrograph (*UH*); *Q*, total runoff.

state variables and model parameters, the latter (i.e., X_1 and/or X_3) can be included in the state vector, according to the augmented state vector approach (Section 3.3.4).

Because in this application there is an exact match between observations and their model equivalent (i.e., streamflow at the catchment outlet), the hydrological model serves as a forward model in the EnKF scheme. Indeed, the GR5J model is used to map inputs to states and also to map states to observations. Error covariances are sampled from the ensemble and not explicitly formed (Evensen, 2003):

$$P_t H^T = \frac{1}{nens-1}\sum_{i=1}^{nens}\left(x_{t,i}^b - \overline{x}^b\right)\left(H\left(x_{t,i}^b\right) - H\left(\overline{x}^b\right)\right)^T \quad (5)$$

$$HP_t H^T = \frac{1}{nens-1}\sum_{i=1}^{nens}\left(H\left(x_{t,i}^b\right) - H\left(\overline{x}^b\right)\right)\left(H\left(x_{t,i}^b\right) - H\left(\overline{x}^b\right)\right)^T \quad (6)$$

where *nens* is the number of ensemble members and the overline denotes an average over the ensemble. $P_t H^T$ is the *nstate* × *nobs* matrix of covariance between the model states and the modeled streamflow, and $HP_t H^T$ is the *nobs* × *nobs* matrix of model covariance at the gauging sites. It is noteworthy that in this lumped application discharge measurements are assimilated at catchment scale (i.e., *nobs* is equal to 1).

The SIR-PF scheme (Figure 4) relies on a stratified resampling (Kitagawa, 1996), which guarantees an ease of implementation and a low computational complexity (Douc & Cappé, 2005). Particle weights are recursively updated at each assimilation time step, as a function of the likelihood of the ensemble streamflow values with respect to the observed discharge. Importance weights are initialized by assigning uniform importance weights to the ensemble particles. Whenever an undesired ensemble shrinkage hinders an efficient resampling procedure, due to the resulting almost equivalent likelihood values, the particle weights are assigned uniformly to prevent possible misleading updated states.

3.3.2. Constrained EnKF Analysis

Unlike the PF, the EnKF acts directly on the state variables of each ensemble member in the analysis procedure through a corrective term accounting for the uncertainty affecting both model predictions and observations. Hence, proper mass constraints are required to prevent possible inconsistencies that may occur owing to unfeasible values of model states resulting from the filter update. Possible inconsistent values of model states are likely to lead to unreliable streamflow simulations especially when the predicted streamflow is significantly different from the observed value (Maxwell et al., 2018). This downside is not experienced with the PF, which preserves the state consistency of each particle through the weighting and resampling procedure. When implementing the EnKF scheme in the GR5J model, mass constraints are required to guarantee the non-negativity of state variables (i.e., storage levels) by ensuring minimum state values. A further constraint is required to prevent the level of the production store from exceeding its maximum capacity. With the aim of training the filter on the threshold-based store parameterization, this latter constraint is also applied to the routing store, even though it may take higher levels than its capacity.

A mass constraint is applied before the forecast step, so that the level of production store (S) cannot drop below 5 % of its capacity (X_1). This constraint is needed to prevent numerical instabilities within the evaluation of the covariance matrices, as the store level drops to values close to zero in the case of low flow. However, under this condition, the constraint on the minimum store threshold is likely to undermine the forecast reliability owing to the generation of possible spurious baseflow rates. It is noteworthy that this undesired issue does not affect the analysis of this study, as it occurs only in few watersheds during summertime. When

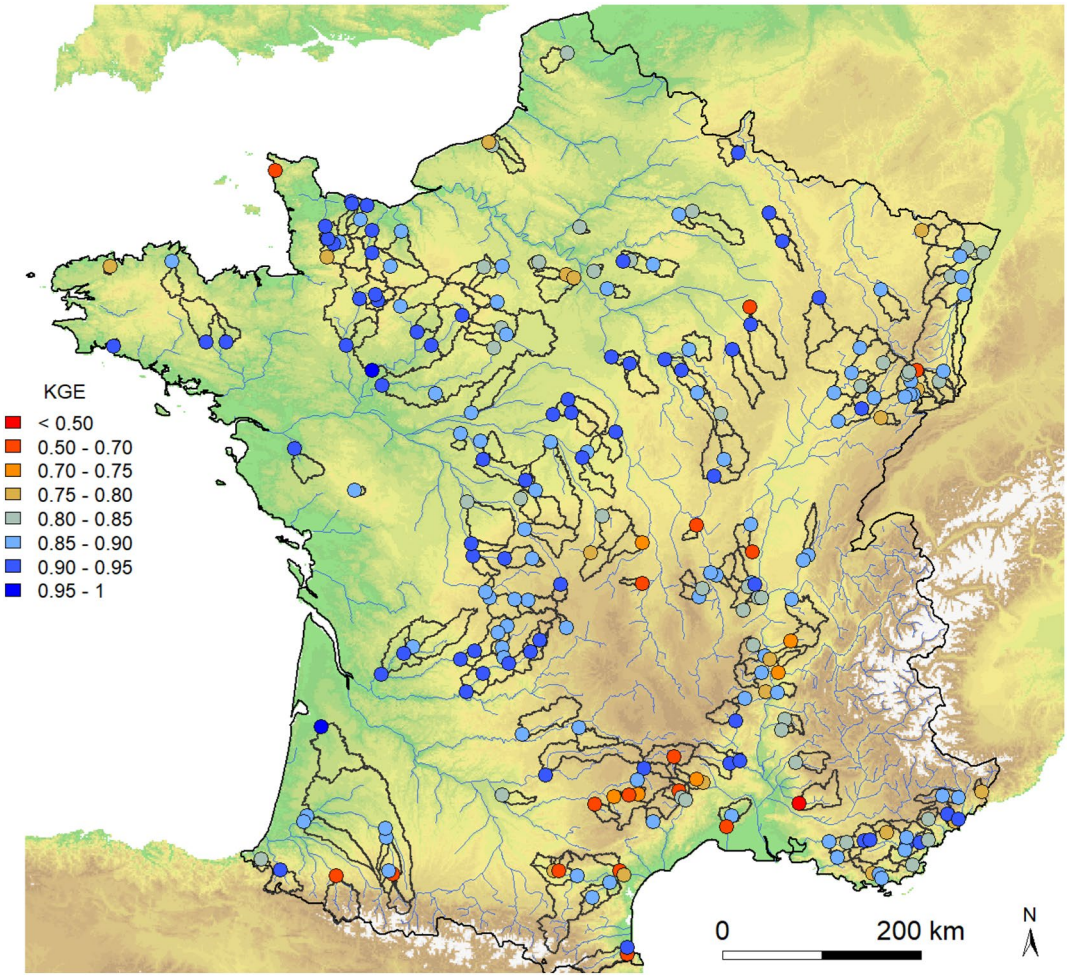

Figure 2. Map showing the location of the 232 French basins and measurement stations used in this study. KGE values resulting from GR5J calibration are reported. KGE, Kling–Gupta efficiency.

performing the joint state–parameter estimation, the store capacities are also limited to positive values. It is noteworthy that the same set of constraints is also used to prevent possible inconsistent values of state variables resulting from their perturbation (Section 3.3.4), which may compromise prediction reliability. Threshold-based control has been shown not to significantly distort the null-valued mean of perturbations.

3.3.3. Uncertainty in Meteorological Forcings

When dealing with ensemble-based DA techniques, the scale of spread of the ensemble simulations is one of the main critical issues. In the PF scheme, the most conducive condition calls for well-spread ensembles. Indeed, when the ensemble is squeezed, the resampling procedure is more challenging, since all the particles are close to each other, resulting in similar likelihood values. In this undesired case, the filter might not succeed in effectively discriminating the more likely ensemble members, since they are all assigned almost the same weight. On the other hand, if the particles are well spread, their resampling is more straightforward, since each particle is properly discriminated through a specific weight proportional to its likelihood. Because the EnKF quantifies the model error based on the variance between ensemble members, poor variance can affect the updating procedure by leading to overweighting the predicted states and weakly assimilating the observed ones. Conversely, an overly broad ensemble spread can lead to an overconfidence in observations, regardless of their reliability. Therefore, an effective representation of all different uncertainties from meteorological forcings, model parameters and states, and observations is a crucial issue in DA. In order to properly take into account, the uncertainty of meteorological inputs, probabilistic meteorological forecasts are generated by stochastically perturbing the model forcings, namely, precipitation

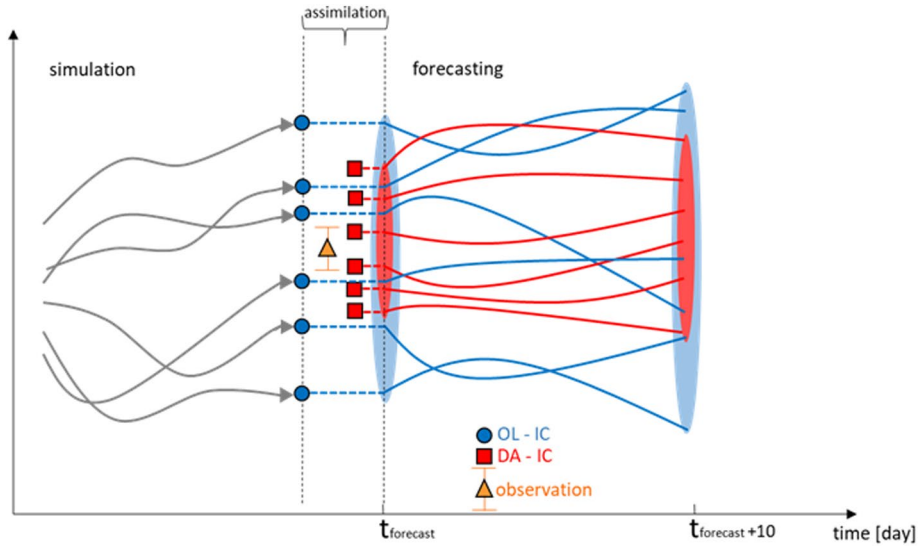

Figure 3. Scheme of the forecasting system. The simulated initial conditions (OL-IC) are updated through assimilation (DA-IC).

and potential evapotranspiration. This approach makes it possible to rely on a well-representative range of weather scenarios.

Ensemble meteorological forecasts are generated by perturbing in situ meteorological observations with multiplicative stochastic noise applied at each time step (i.e., daily), according to the methodology proposed by Clark et al. (2008). The random perturbations are provided by a first-order autoregressive model in order to guarantee physical consistency and temporal correlation of the time-variant forcings. Indeed, this approach accounts for time-variant model errors, which are supposed to be more representative of model uncertainty than temporally constant ones. To generate perturbations of both meteorological variables, the fractional error parameter is set to 0.65 and the temporal decorrelation length is defined as 1 day for rainfall and 2 days for potential evapotranspiration.

3.3.4. Uncertainty in Model Parameters and State Variables

Of the several uncertainties affecting hydrological predictions, meteorological forcings are among the most relevant. However, perturbation of the meteorological data alone is unlikely to comprehensively represent system uncertainties, especially during drought periods. Indeed, when no precipitation events occur, the spread of the ensemble hydrological simulations is generally greatly reduced (Figure 5).

In order to prevent ensemble shrinkage, even in the absence of precipitation, further uncertainties can be represented through the introduction of additional stochastic noise. Indeed, while the perturbation of meteorological forcings accounts for uncertainties in model input, the perturbation of model states and parameters allows for a representation of the uncertainty in the model itself (Clark et al., 2008; Reichle et al., 2002).

According to the methodology proposed by Moradkhani, Hsu, et al. (2005), at each assimilation time step after the analysis procedure, both model states (Figure 6) and parameters (Figure 7) can be perturbed through normally distributed null-mean noise. The noise variance is assumed equal to the variance of the internal variables resulting from the analysis procedure. However, in order to avoid model instabilities due to large changes in the perturbed internal variables and to assure minimum process noise by preventing ensemble collapse, variance is restricted between upper and lower limits (Salamon & Feyen, 2009).

In order to properly set the variance ranges, several tests were performed to assess the sensitivity of the DA performance to different limit values of the noise variance. Each test was repeated several times by varying the variance ranges for each internal variable and evaluating the impact on filter performance over the longest possible analysis period according to the available discharge observations at each basin. The initial variance ranges for each internal variable were defined starting from the assessment of the annual

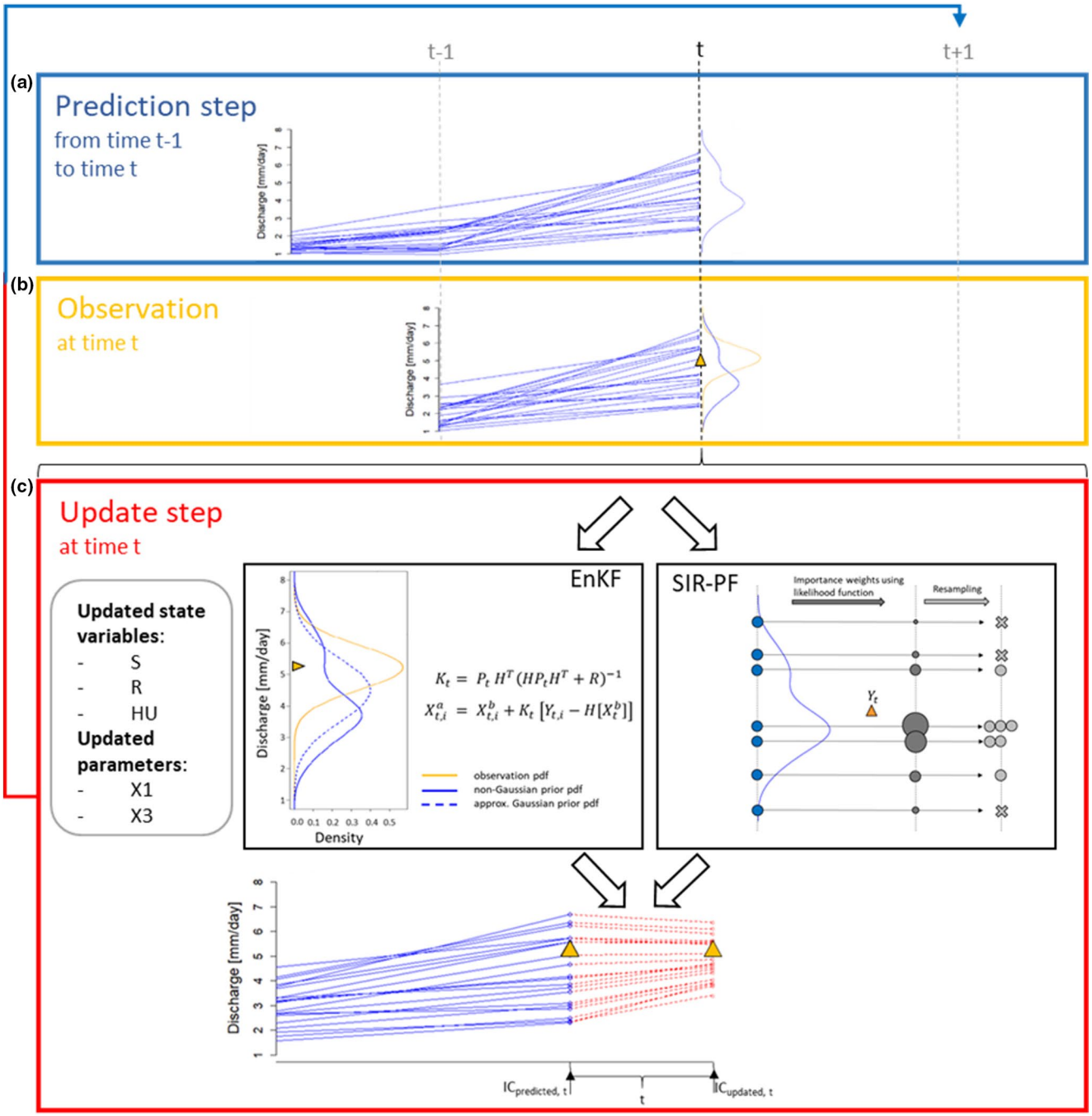

Figure 4. Schematic representation of the sequential data assimilation (DA) algorithms. The prediction step (a) provides an ensemble of a priori estimates of model states (i.e., the blue dots; the blue curve is the non-Gaussian prior distribution). When an observation Y is available (b) (i.e., the orange triangle; the orange curve is the Gaussian observation error distribution), it is assimilated within the update step (c) to estimate the analysis state. The ensemble Kalman filter (EnKF) assumes a Gaussian prior distribution (i.e., the blue dashed curve) to evaluate the Kalman gain (K_t) and the analysis states $\left(X_t^a\right)$. In the particle filter (PF) scheme, the importance weights are updated according to the likelihood value of each particle with respect to the observation. The sizes of the particles (dark gray circles) are proportional to their weights. In the resampling procedure, samples with negligible weights are removed (light gray crosses), while samples with large weights are replicated (light gray circles) to restore ensemble size and to avoid filter degeneracy. Because this is a sequential DA scheme, the propagated model analysis states (i.e., the red dots) resulting from the update step t (c) are the initial states at the following prediction time step $t + 1$ (a).

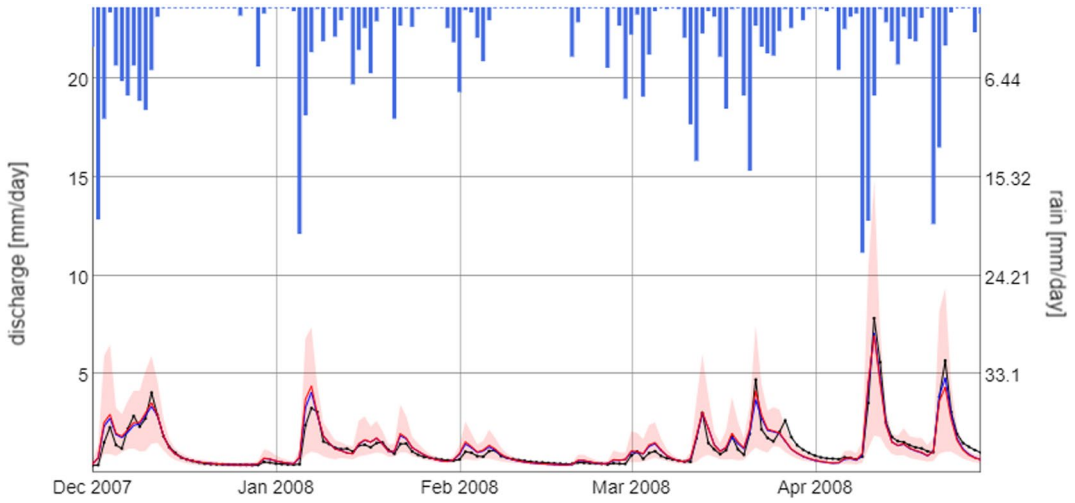

Figure 5. Ensemble streamflow simulation accounting for meteorological uncertainty. The ensemble mean and spread are shown in red, and the OL discharge simulation is shown in blue.

variability of each state variable throughout the whole analysis period and the variability of model parameters over all the selected basins. It is noteworthy that all the tests were performed for a given observation error (see Section 3.3.5).

A sensitivity analysis allowed selection of the parameters exerting the most influence on model simulations, namely, the capacities of the production (X_1) and routing (X_3) stores. This preliminary study was performed by making the parameters vary within proper ranges and analyzing the impact of their variation on the

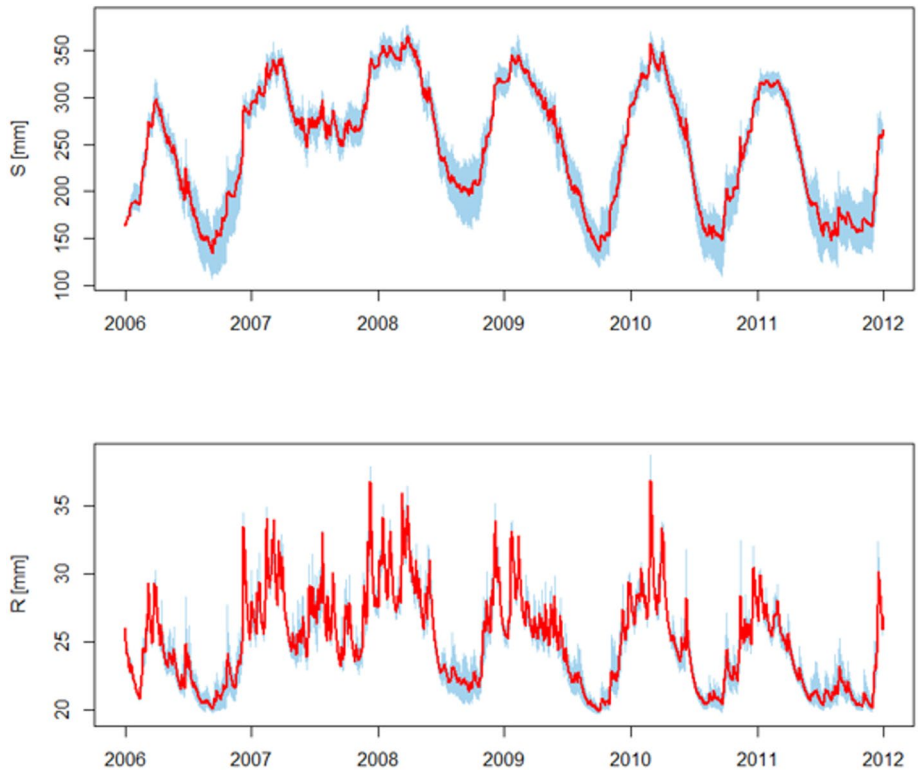

Figure 6. An example of DA-based ensemble simulations of the levels of both the production (S) and routing (R) stores for the Avre River (watershed of 495 km^2). The ensemble mean is reported in red, the ensemble spread in light blue.

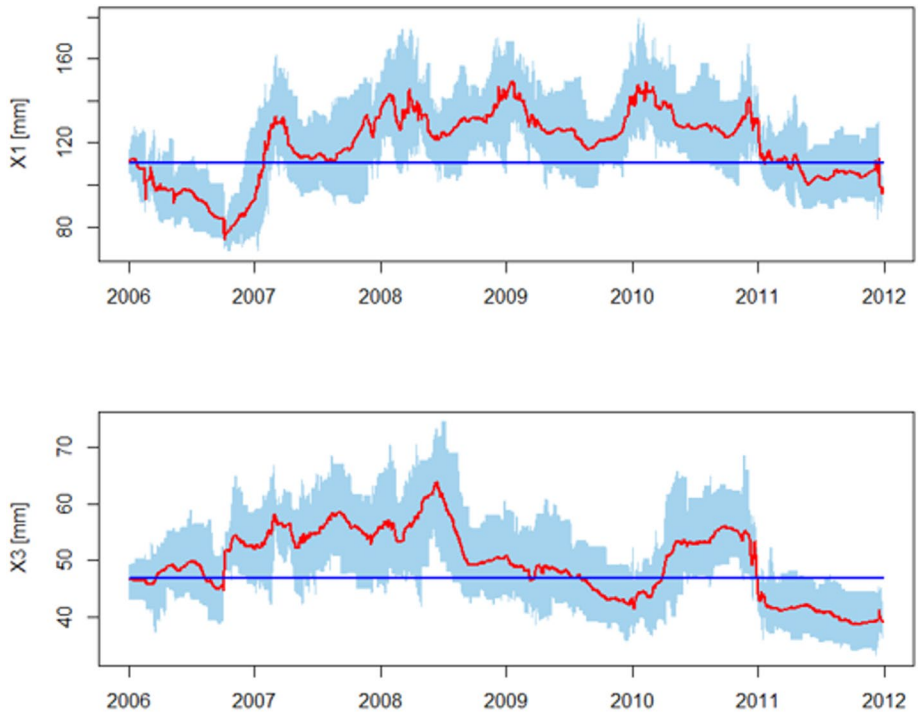

Figure 7. An example of DA-based ensemble simulations of the capacities of both the production (X_1) and routing (X_3) stores for the Célé River (1,194 km^2). The ensemble mean is reported in red, the ensemble spread in light blue.

resulting model predictions. Parameter ranges were estimated in order to avoid model numerical instabilities and to comply with possible constraints (from 0.01 mm to 5,000 mm for the production store and 2,000 mm for the routing store).

Since the dual estimate (Moradkhani, Sorooshian, et al., 2005) entails a higher computational time and both the limited system dimensionality and the small number of model states and parameters reduce the occurrence of possible spurious correlations (Xie & Zhang, 2013), the augmented state vector approach is applied to the GR5J model in this study.

3.3.5. Observational Uncertainty

While it is of key importance to ensure a well-spread ensemble to properly represent model uncertainties, it is also critically important to estimate the observation error, since this defines how the filter trusts the observations and, thus, to what extent they are assimilated into the model. The uncertainty in discharge observations is mainly due to the instrumental error and the uncertainty in the rating curve (Clark et al., 2008). In this study, measurement noise is generated from a normal distribution with a zero-valued mean and a variance (σ^2_{obs}) parameterized as a function of the observed streamflow rate (Q_{obs}) (Clark et al., 2008; Weerts & El Serafy, 2006):

$$\sigma^2_{obs} = \left(\varepsilon_{obs}\, Q_{obs}\right)^2 \tag{7}$$

According to preliminary analyses assessing the sensitivity of filters to the observation error, the error parameter ε_{obs} was set to 0.1. In order to prevent underestimated error variances in the case of low discharge, the quantile 10 (Q_{10}) of streamflow observations was assumed as the minimum threshold value to define the error variance. Indeed, following the approach proposed by Thirel et al. (2010), for streamflow values below Q_{10}, the variance is evaluated proportionally to Q^2_{10}.

3.4. Experimental Setup

Several experiments are performed with the aim of assessing both the benefit of updating different model states and parameters and the impact of considering several sources of uncertainty when estimating more accurate DA-based forecast ICs. Indeed, the main purpose is to identify the critical uncertainties to be taken into account and the key model states and parameters to be updated via DA to efficiently improve the forecasting skill of a conceptual rainfall–runoff model. Furthermore, the performance of the EnKF and PF schemes is assessed and compared in terms of both forecasting accuracy and temporal persistence of the updating effect.

Table 1 lists all the experiments. "A" experiments aim at assessing the usefulness of updating the state variables (i.e., S, R, UH stocks) when considering only the uncertainty of the meteorological forcings (Section 3.3.3). In order to identify the most relevant state variables, namely those model states that guarantee the largest improvement of the forecast ICs if updated, the benefit achieved through the EnKF-based update of each state variable is evaluated (Exps. A2, A3, A4). For instance, the experiment EnKF_A3 assesses how the EnKF-based update of the initial level of the routing store (R) impacts the forecasting skill when accounting for meteorological uncertainty. Therefore, in this case, the state vector includes only R (Section 3.3.1).

"B" experiments are designed to investigate the potential of jointly updating both state variables and model parameters (i.e., X_1, X_3). In addition to meteorological uncertainty, these experiments (Exps. B1–B3) also take account of the uncertainty in the parameter estimation (Section 3.3.4). For example, the experiment PF_B1 aims to evaluate the impact on the accuracy of the forecast ICs when the initial level of the production store (X_1) is jointly updated together with all the state variables by allowing for the uncertainty of the X_1 estimate as well as meteorological perturbations. Consistently, the state vector encompasses S, R, UH and X1 in that case.

"C" experiments aim to assess whether the introduction of the uncertainty of the state variables (Section 3.3.4) can affect the DA-based update of the forecast ICs and the resulting impact in terms of predictive skill. Consistent with A experiments, also in this case, the most relevant state variables are investigated in the experiments C2–C4.

According to the experimental setup (Table 1), in each experiment the ensemble of model states is generated by introducing some system noise through the stochastic perturbation of specific variables. To properly initialize the ensemble, all experiments rely on a one-year model warm-up period just preceding the start of the analysis period. According to the results of a preliminary analysis of sensitivity to the ensemble size, all the experiments rely on an ensemble of 100 members, which guarantees stable performance for both the DA schemes in this application to a lumped conceptual model. It is noteworthy that the PF generally reveals higher sensitivity to the ensemble size than the Kalman filter. Furthermore, to consistently compare the two analyzed DA techniques, the same noise statistics are used in all experiments.

3.5. Evaluation Metrics

In order to ensure a proper comparison of the performance of the EnKF and PF schemes, the evaluation metrics are computed against the OL probabilistic predictions, which are assumed as the benchmark in all experiments to assess updating effects.

To avoid possible misevaluation, over and underevaluation, both deterministic and probabilistic verification metrics are evaluated for each lead time to properly analyze the different attributes of streamflow forecasts (Anctil & Ramos, 2018). The root mean square error (RMSE) is evaluated for the single-valued ensemble mean forecast, with the aim of evaluating model accuracy (lower values indicate better forecasts).

The overall accuracy of DA-based forecasts is assessed against the accuracy of OL predictions by evaluating the continuous ranked probability skill score (CRPSS) (R package *verification*; NCAR Research Applications Laboratory, 2015), according to the formula:

$$CRPSS = 1 - \frac{CRPS}{CRPS_{OL}} \tag{8}$$

Table 1
Experiment Notes

Experiment ID	Exps. A		Exps. B		Exps. C	
Updated variables	ICs		ICs and parameters		ICs	
Uncertainty	Met. Inputs		Met. inputs and model parameters		Met. inputs and model states	
	EnKF	PF	EnKF	PF	EnKF	PF
1	S, R, UH	S, R, UH	S, R, UH, $\mathbf{X_1}$	S, R, UH, $\mathbf{X_1}$	**S, R, UH**	**S, R, UH**
2	S	-	S, R, UH, $\mathbf{X_3}$	S, R, UH, $\mathbf{X_3}$	**S**	**S**, R, UH
3	R	-	S, R, UH, $\mathbf{X_1}$, $\mathbf{X_3}$	S, R, UH, $\mathbf{X_1}$, $\mathbf{X_3}$	**R**	S, **R**, UH
4	UH	-	-	-	**UH**	S, R, **UH**

Note. Updated variables are listed for each experiment; perturbed variables are given in bold. All experiments rely on the same ensemble of perturbed meteorological observations.

Abbreviations: EnKF, ensemble Kalman filter; Exps., experiments; ICs, initial conditions; ID, identification; Met., meteorological data; PF, particle filter; R, routing store level; S, production store level; UH, unit hydrograph state; X1, production store capacity; X3, routing store capacity.

where the continuous ranked probability score (CRPS) measures the quadratic distance between the cumulative distribution of the forecasts and the cumulative distribution of the observations of the predicted variable (Hersbach, 2000). A CRPSS value closer to 1 is preferred, since this indicates a lower CRPS value than the reference OL value ($CRPS_{OL}$).

To investigate the reliability of the DA-based forecasts in discriminating between events and nonevents, the so-called area under the receiver operating characteristics (ROC) curve (AUC) is analyzed (R package *ROCR*; Sing et al., 2005), which is a comprehensive summary measure of the discrimination capability of the forecast. AUC values range between 0 (i.e., no distinction between event and no event) and 1 (i.e., perfect score), where a value of 0.5 identifies no skill (Yesilnacar, 2005). In order to evaluate ROC curves and the resulting AUC values, the 90th quantile of the time series of the observed discharges is considered as the overflow threshold, enabling one to identify the occurrence of an event.

4. Results

4.1. The Impact of Meteorological Uncertainty on DA-Based Forecasts

The A experiments aim to assess the usefulness of DA-based estimation of forecast ICs to improve predictive accuracy, when accounting for the uncertainty of the meteorological forcings. The EnKF-based forecasts (EnKF_A1) outperform the PF-based ones (PF_A) in terms of predictive accuracy (RMSE) up to a 3-day lead time (Figure 8). However, it is noteworthy that the PF-based estimates of forecast ICs guarantee a longer-lasting improvement of forecasting skill compared to the EnKF-based updating effect, which decreases more sharply in the short term.

In terms of CRPSS, the estimation of forecast ICs benefits the most from the EnKF-based update of the initial level of the routing store (EnKF_A3), with a resulting improvement in forecast accuracy up to 5 days compared with the reference (OL) (Figure 9). A much lower improvement is achieved by updating the initial level of the production store (EnKF_A2), which does not succeed in efficiently improving forecast accuracy compared to OL predictions. It is noteworthy that the forecasting system reveals negligible sensitivity to updating of the unit hydrograph state (EnKF_A4), as the quantities of water stored in unit hydrographs are much lower than in model stores. The evaluation of CRPSS values reveals the poor usefulness of the PF-based estimate of forecast ICs to enhance predictive accuracy compared with the OL probabilistic forecasts, even for the very short lead time (Figure 9).

In terms of AUC, the forecasting system succeeds in properly discriminating the occurrence of threshold-exceeding events, even without relying on updated forecast ICs (Figure 10). Both EnKF- and PF-based

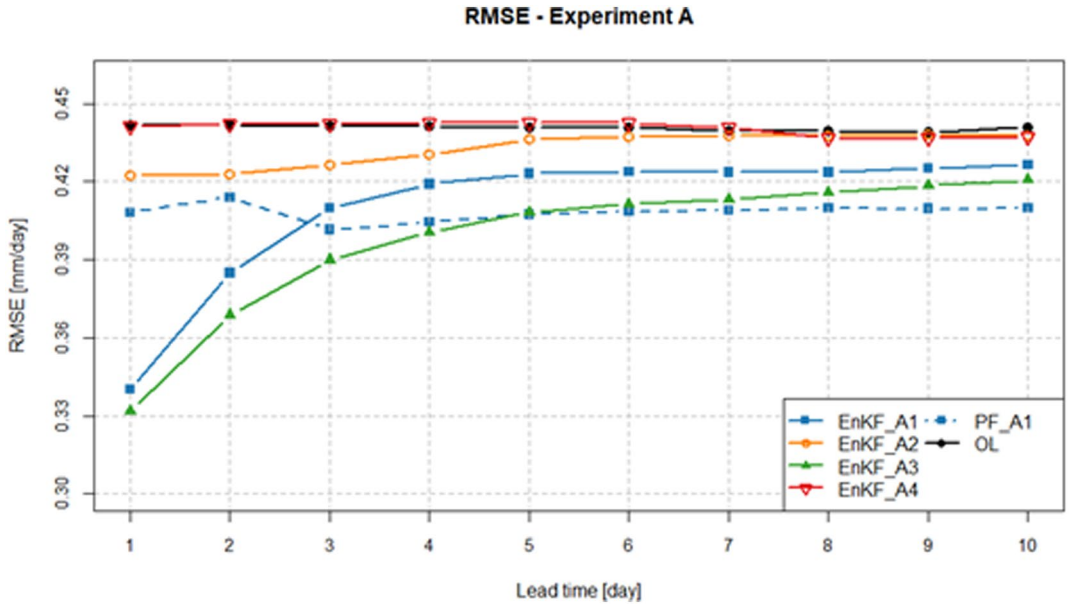

Figure 8. Experiments A: trends in median root mean square error (RMSE) values of the ensemble mean discharge forecasts, evaluated over all the gauging stations for lead times ranging from 1 to 10 days. OL, open loop; PF, particle filter; EnKF, ensemble Kalman filter.

estimates of forecast ICs (EnKF_A1, PF_A) improve the event discrimination capability up to a 6-day lead time. The most benefit in terms of AUC values stems from the EnKF-based estimation of the initial level of the routing store (EnKF_A3).

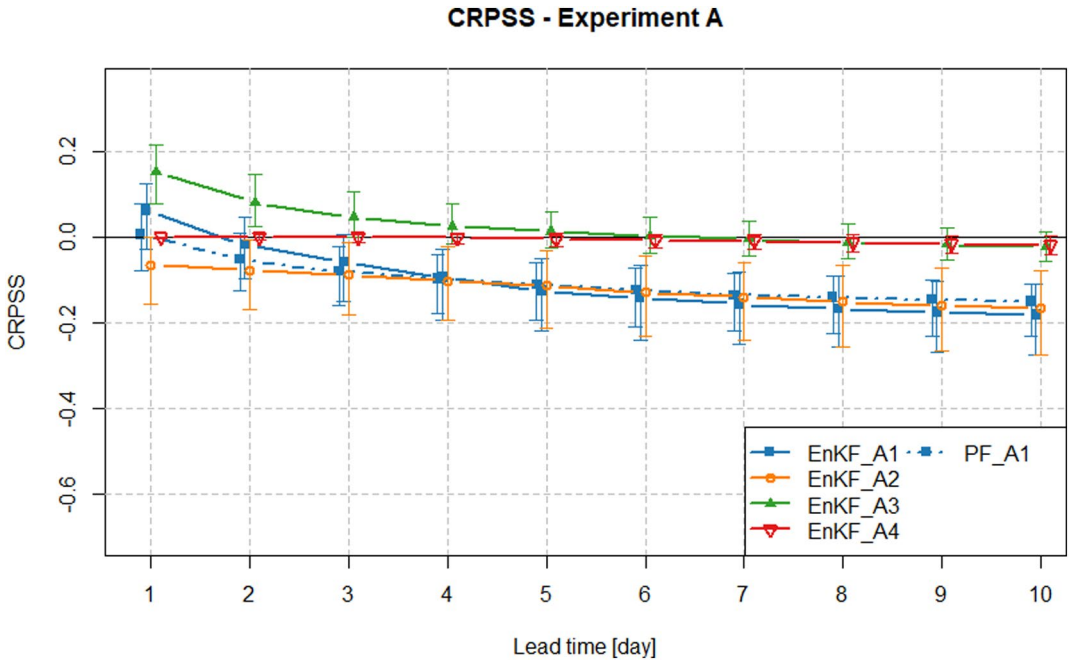

Figure 9. Experiments A: trends in median continuous ranked probability skill score (CRPSS) values of discharge forecasts, evaluated over all the gauging stations for lead times ranging from 1 to 10 days. The upper and lower whiskers are the 25th and 75th percentiles of CRPSS values, respectively. PF, particle filter; EnKF, ensemble Kalman filter.

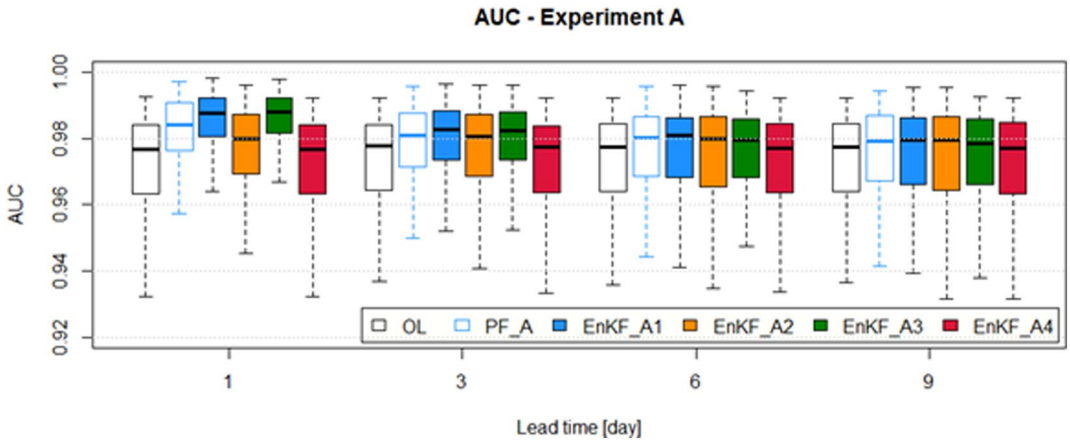

Figure 10. Experiments A: boxplot of area under the curve (AUC) values for all the gauging stations at lead times of 1, 3, 6, and 9 days. OL, open loop; PF, particle filter; EnKF, ensemble Kalman filter.

4.2. The Usefulness of the Joint DA-Based Estimation of Forecast Initial States and Parameters

The main purpose of the B experiments is to assess the benefit of the DA-based update of both model states and parameters through their combined estimation to provide more accurate forecast ICs. The DA-based estimation of the capacity of the production store at the forecast time (Exp. B1) does not result in any significant further improvement in predictive accuracy compared with the previous experiments. Conversely, the forecasting system reveals high sensitivity to the initial capacity of the routing store (Exp. B2), as its updating results in differing performance of the two analyzed DA schemes. Compared to experiment EnKF_A1, the joint estimation of the initial routing capacity (EnKF_B2) allows for higher predictive accuracy in the very short term, with a negligible benefit of the updating effect even at a 2-day lead time (Figure 11). Conversely, the PF-based estimation of the initial capacity of the routing store (PF_B2) significantly undermines forecast reliability due to suboptimal ICs, compared to OL predictions.

4.3. The Impact of State Uncertainty on DA-Based Forecasts

The C experiments are focused on the impact of state uncertainty on the DA-based estimation of the forecast ICs, in terms of both forecasting accuracy and temporal persistence of the updating effect. Consistent with the results of A experiments, the EnKF-based forecasts benefit the most from the updating of the initial level of the routing store (EnKF_C3), in terms of RMSE (Figure 12). Even though the uncertainty in the estimate of the routing store level allows for a larger improvement of forecast ICs compared to the EnKF_A3 experiment, the accuracy of the EnKF-based forecasts decreases even more sharply within a 3-day lead time compared with the PF-based ones. Conversely, state uncertainty undermines the accuracy of forecast ICs through the DA-based estimate of the production store level (EnKF_C2). Updating the unit hydrograph state (EnKF_C4) still does not improve forecasting skill, even when accounting for state uncertainty.

PF-based forecasts reveal consistent sensitivity to state uncertainty in terms of predictive accuracy. Indeed, compared with the PF_A experiment, the accuracy of forecast ICs is more efficiently improved when accounting for uncertainty in the estimate of the initial level of the routing store (PF_C3). While uncertainty in the estimate of the unit hydrograph state allows for slightly more accurate forecast ICs (PF_C4), forecasting skill is undermined when accounting for uncertainty of the production store level (PF_C2). It is noteworthy that the EnKF (EnKF_C1) outperforms the PF (PF_C1) in terms of RMSE, especially in the short term, by providing more accurate forecast ICs.

The assessment of CRPSS values stresses the key benefit of accounting for the uncertainty in the initial level of the routing store, which guarantees the most efficient improvement of IC accuracy up to a 5-day lead time through the PF-based update of model states (PF_C3) (Figure 13). When taking account of the uncertainty of all states, the PF-based forecasts (PF_C1) outperform the EnKF-based ones (EnKF_C1), as they allow for the highest forecasting accuracy compared to the reference OL predictions.

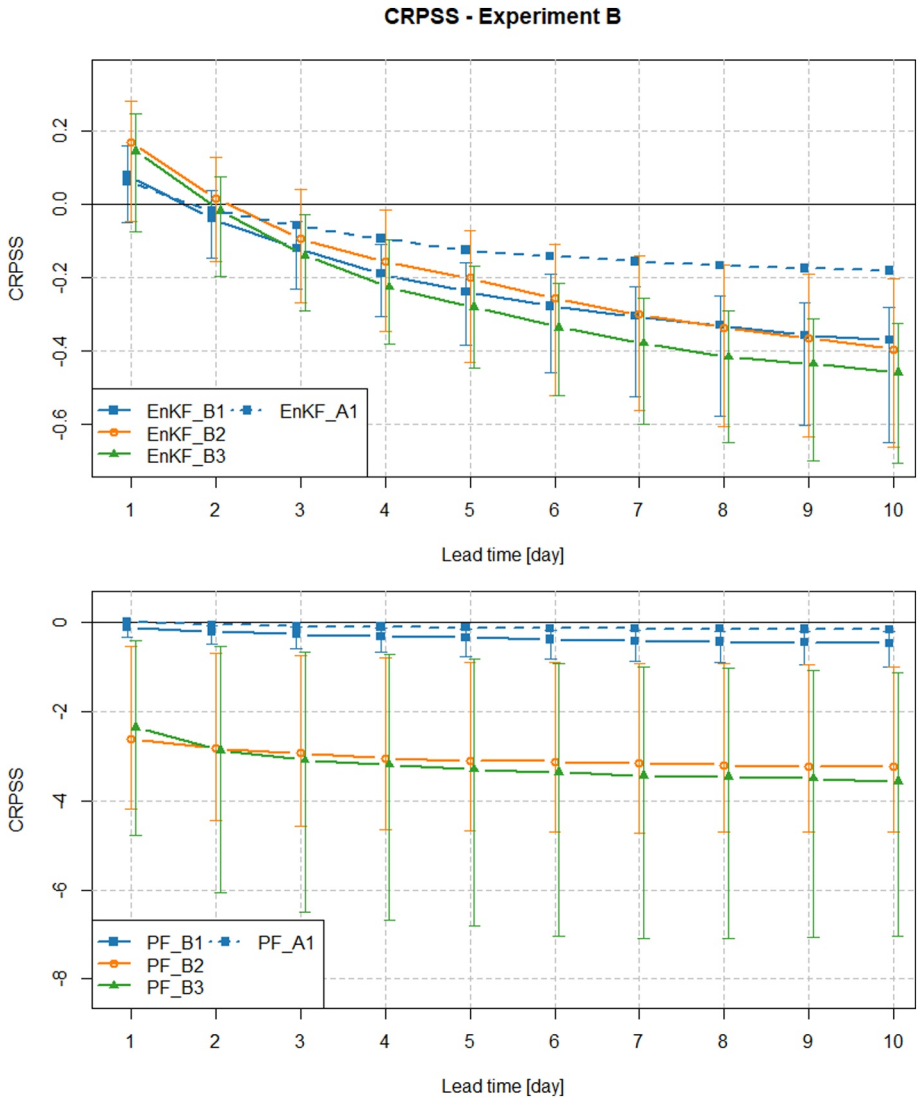

Figure 11. Experiments B: trends in median continuous ranked probability skill score (CRPSS) values of discharge forecasts, evaluated over all the gauging stations for lead times ranging from 1 to 10 days. As reference, experiments A are reported as dotted lines. EnKF, ensemble Kalman filter; PF, particle filter.

Compared with the A experiments, the event discrimination capability of the forecasting system is significantly enhanced through both the PF- and EnKF-based estimation of forecast ICs, accounting for the uncertainty of the routing store level (PF_C3, EnKF_C3), especially in the short term (up to a 4-day lead time) (Figure 14). Conversely, no further improvement can be inferred from the AUC values of the DA-based forecasts relying on the uncertainty of the other two state variables.

4.4. The Impact of DA-Based Updating Procedures on Model States

Compared to the PF, the EnKF reveals a higher rate of accuracy decay with increasing lead time. According to Dumedah and Coulibaly (2013), the more steady accuracy of PF-based forecasts suggests that the sequential updates of model internal variables are not overly disruptive. Conversely, the introduction of new observed information in the EnKF scheme can overwhelm the background knowledge or overly drive the assimilation towards itself. The limited performance of the EnKF is mainly related to the update of the state variables by using linear updating rules based on covariance information of both model states and observations (Noh et al., 2013). The Gaussian approximation can result in a suboptimal estimation of the filtering

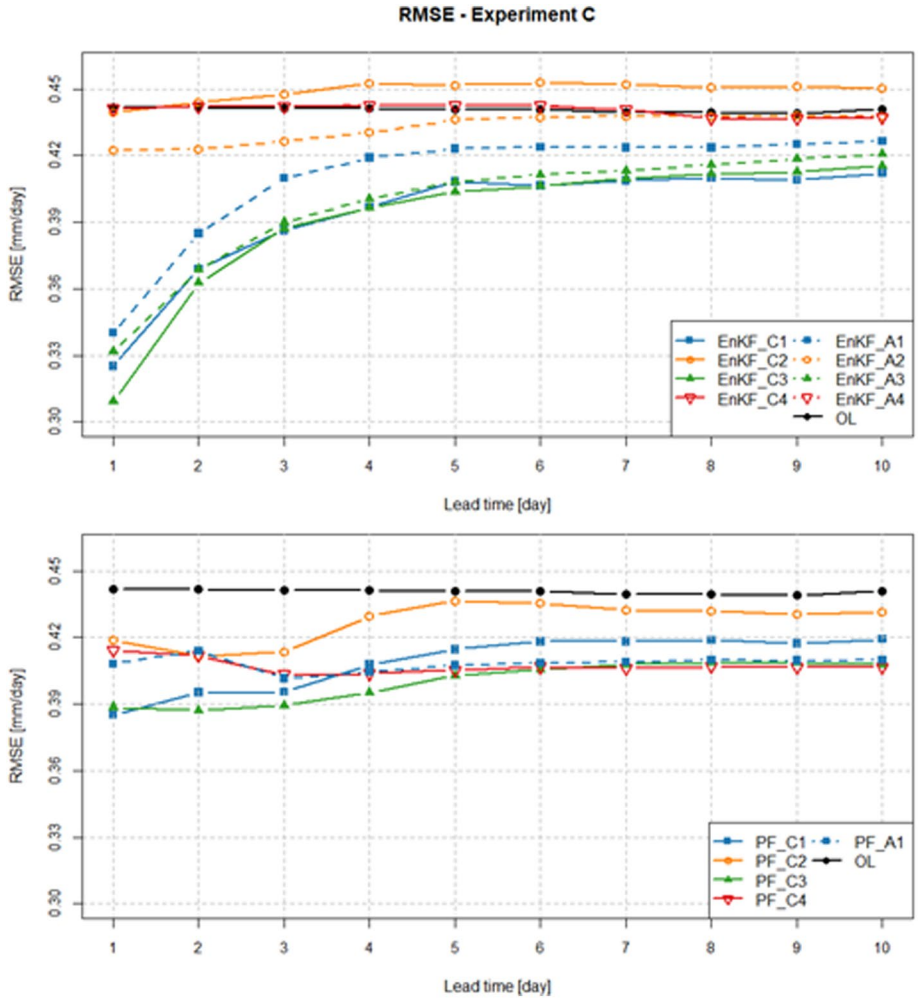

Figure 12. Experiments C: trends in median root mean square error (RMSE) values of the ensemble mean discharge forecasts, evaluated over all the gauging stations for lead times ranging from 1 to 10 days. OL, open loop; EnKF, ensemble Kalman filter; PF, particle filter.

probability density function, which is likely to lead to possible inconstancies affecting the updated state of the realizations (Pasetto et al., 2012).

Even though the GR5J model is not strongly nonlinear, the low correlation between discharge measurements and some of the state variables can hinder the EnKF from properly retrieving these latter. Therefore, a rapid decline of the predictive accuracy of EnKF-based forecasts can occur when forecasting for longer lead times.

Unlike the EnKF, all information in the ensemble is duplicated in the PF resampling step, which prevents numerical instabilities and increases forecasting accuracy (Noh et al., 2013). Indeed, in the update step the PF duplicates the realizations that are closer to the observations and thus it preserves both the system mass balance and the overall state consistency of each particle (Noh et al., 2018), instead of directly correcting the internal variables based on the discharge residuals.

Because the difference in the temporal persistence of the EnKF- and PF-based updating effect is supposed to be mainly related to the different analysis procedure of these two DA techniques, the impact of DA-based updates on model states (i.e., levels of production and routing stores) is assessed. The two sequential DA techniques are compared by evaluating the differences between the background and analysis states resulting from both the updating procedures. As expected, Figure 15 shows that the PF-based analysis procedure

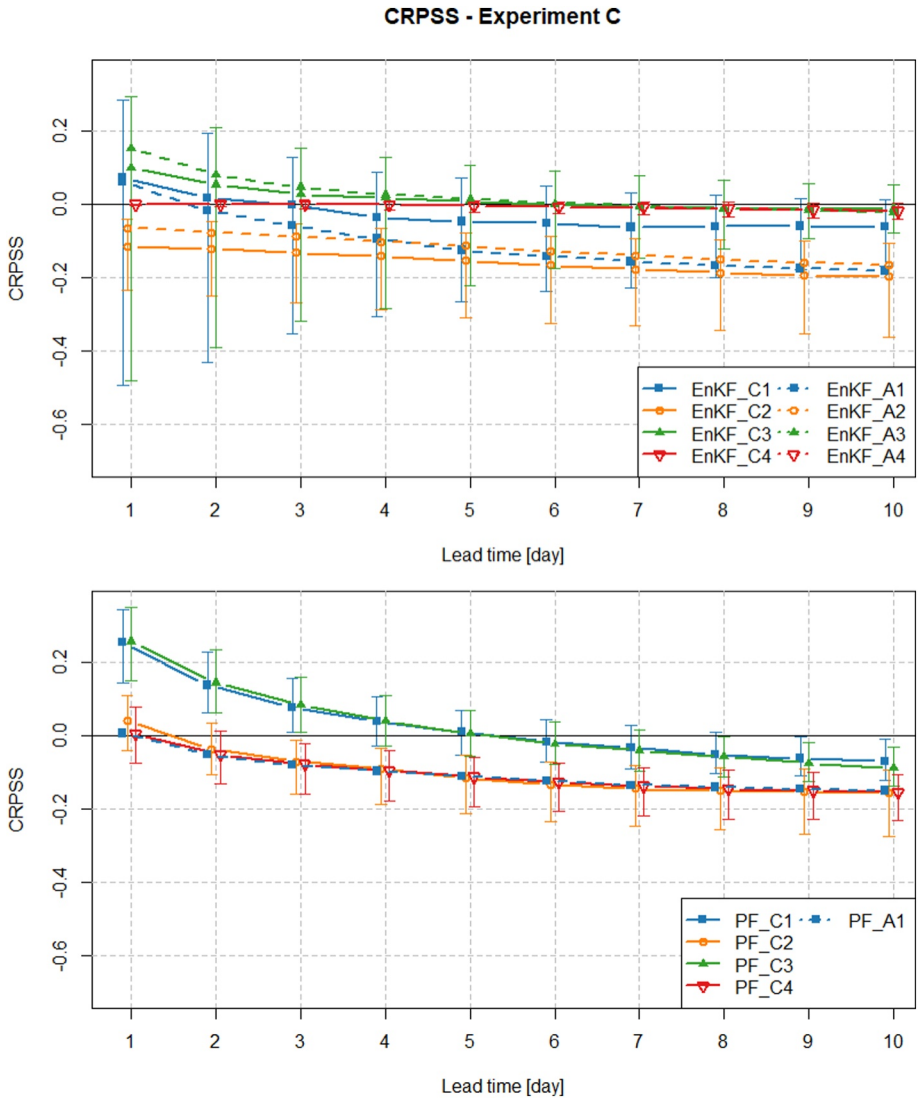

Figure 13. Experiments C: trends in median continuous ranked probability skill score (CRPSS) values of discharge forecasts, evaluated over all the gauging stations for lead times ranging from 1 to 10 days. As reference, experiments A are reported as dotted lines. EnKF, ensemble Kalman filter; PF, particle filter.

generally results in smaller updates of state values than the EnKF scheme, especially for the production store (S).

Although larger correction terms result in a more effective update of model states, they are more likely to lead to possible inconsistencies in the resulting values of state variables, in spite of proper mass constraints (Section 3.3.2) and limited system perturbations. Consequently, the persistence of the updating effect can be significantly reduced, since the model tends to restore state variables consistent with the model physics. On the other hand, even though a weaker update of state variables leads to poorer filter efficiency in improving forecast ICs, it generally lasts longer over the forecast horizon.

5. Discussion

Compared with PF-based forecasts, EnKF-based estimates of forecast ICs guarantee a greater improvement in predictive accuracy in the short term, when accounting only for meteorological uncertainty (Exps. PF_A and EnKF_A1 in Figure 8). Indeed, a noncomprehensive representation of the system uncertainties restricted to only the model forcings undermines the efficiency of the PF-based estimation of forecast ICs.

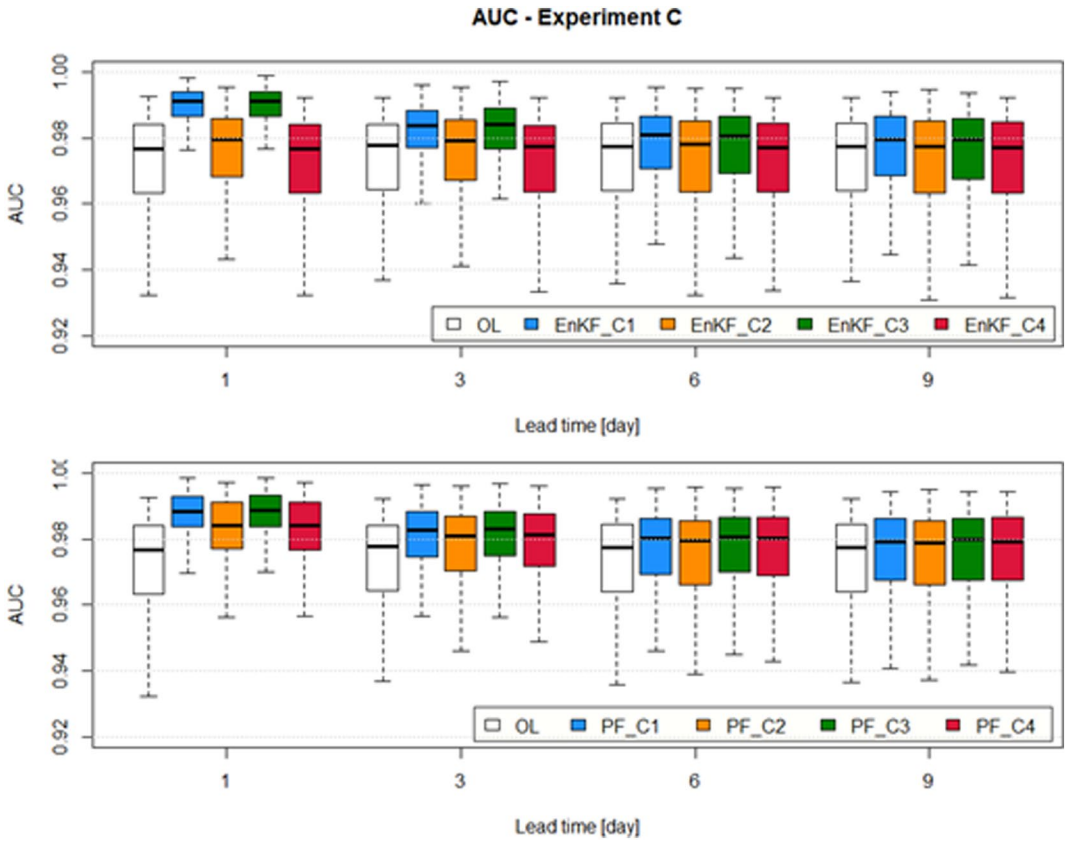

Figure 14. Experiments C: boxplot of area under the curve (AUC) values for all the gauging stations at lead times of 1, 3, 6, and 9 days. OL, open loop; EnKF, ensemble Kalman filter; PF, particle filter.

Especially in no-rain periods, the reduction in the ensemble spread makes the particle resampling procedure more challenging, since the filter might not succeed in effectively discriminating the more likely particles owing to almost equivalent importance weights.

State uncertainty has a different impact on the usefulness of PF- and EnKF-based estimations of forecast ICs, in terms of both efficiency and temporal persistence of the updating effect (Exps. C). A more comprehensive representation of both meteorological and state uncertainties allows for an enhanced benefit of

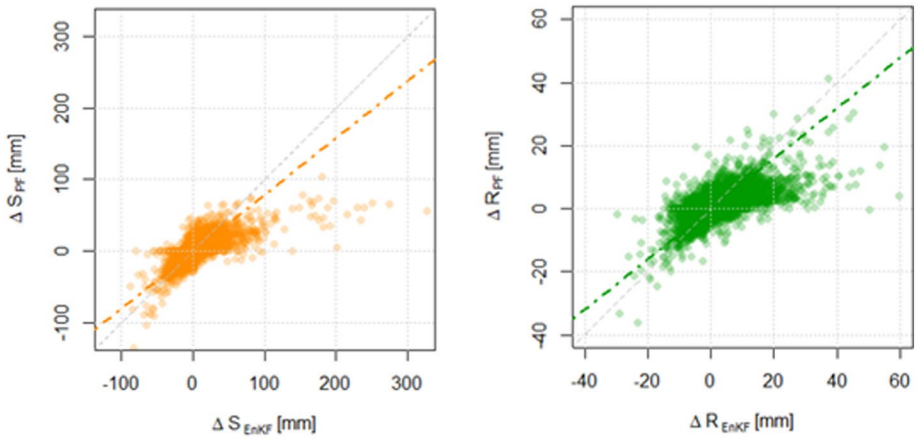

Figure 15. Scatterplot of the differences between background and analysis states resulting from particle filter (PF)- and ensemble Kalman filter (EnKF)-based updating procedures. The dash-dotted lines are the regression lines.

PF-based estimates of forecast ICs (Exps. PF_A1 and PF_C1 in Figure 13). Indeed, a larger spread of the ensemble simulations entails a more straightforward weighting and, thus, more efficient resampling of particles. In the case of the EnKF, higher model error covariance can lead to an overweighting of observations in the analysis procedure.

While the PF-based updating effect is longer lasting over the forecast horizon (Noh et al., 2013), the benefit of larger corrective terms for the EnKF rapidly decreases within a short lead time (Thiboult et al., 2016). The difference in the rate of accuracy decay (Exps. EnKF_C1 and PF_C1 in Figure 12) is mainly related to the different updating schemes of the two DA techniques. Indeed, whenever the Gaussian approximation in the EnKF scheme leads to possible inconsistencies affecting the updated states, the system tends more quickly to restore state variables consistent with the model physics (Pasetto et al., 2012). This issue is likely to be even more recurrent when enlarging the model error covariance by state perturbation (Exps. EnKF_A3 and EnKF_C3 in Figure 13). Hence, mass constraints are needed to prevent possible misleading state values resulting from the EnKF-based update (Maxwell et al., 2018).

Among hydrological processes, routing dynamics has the highest impact on the accuracy of DA-based estimates of forecast ICs (Exp. EnKF_A3 and Exps. C3). Indeed, updating of the forecast initial level of the routing store allows for the most significant improvement in predictive accuracy (Exps. C3 in Figure 13). The DA-based estimate of the production store level is generally less efficient at improving forecasting accuracy (Exp. EnKF_A2 and Exps. C2), since in GR5J model the level of the production store is less correlated with the observed discharge than the routing store level. Therefore, the increase in the ensemble spread due to the uncertainty in the estimate of production store level can even be more counterproductive (Exps. EnKF_A2 and EnKF_C2 in Figure 13). It is noteworthy that the relative importance of the states of the production and routing stores and their different correlation with streamflow observations do not vary consistently with the main topographic (e.g., watershed surface) and hydroclimatic (e.g., hydrologic regime) conditions of catchments.

The DA-based update of the unit hydrograph state at the forecast time (Exp. EnKF_A4 and Exps. C4) cannot be deemed an efficient approach to enhancing streamflow forecasting skill, since the forecasting system generally reveals negligible sensitivity to the estimation accuracy of this variable (Exps. C4 in Figure 13). Indeed, unlike the other state variables (i.e., store capacities), updating the unit hydrograph state concerns only modest water quantities, which are not likely to significantly impact the water balance of the system throughout the forecast horizon.

The DA-based estimation of forecast parameters is a more critical issue, since the forecasting system reveals high sensitivity to parameter uncertainty (Exps. B). Indeed, because store capacities govern the simulated hydrological responsiveness of the basin (see Section 3.2), their DA-based update can significantly modify the system response to meteorological forcings (Exp. PF_B3 in Figure 11). This implies that the parameter values updated by the assimilation of the observed discharge at the forecast time may not be the optimal ones to represent the model response over the entire 10-day forecast horizon. Indeed, the updated parameter values are specifically estimated to optimally fit the available observations up to forecast initialization by adjusting the model response to the prevailing hydroclimatic conditions. Therefore, the analysis values of store capacities can significantly differ from their calibrated values (see Section 3.2) that are used in the OL probabilistic forecasts. Indeed, while the calibrated values of model parameters ensure to optimize the average model responsiveness, their analysis values are generally optimal only close to the forecast time step. This is especially the case with the EnKF-based estimates of forecast parameters, which significantly affect predictive quality over the forecast horizon, even though they succeed in improving forecasting accuracy in the very short term (Exps. EnKF_B3 in Figure 11). The DA-based estimation of production store capacity (Exps. EnKF_B1 and PF_B1 in Figure 11) does not significantly improve predictive accuracy. Indeed, along with its low correlation with the observed discharges, the update of this model parameter is likely to result in a smooth effect on the model hydrological response in the longer term. Conversely, the forecasting system reveals high sensitivity to the updating of routing capacity (Exp. B2), which promptly affects the hydrological response of the model even in the very short term. While the EnKF succeeds in correctly updating this model parameter (Exp. EnKF_B2 in Figure 11), thanks to its higher correlation with the observed discharges, its PF-based estimation is generally suboptimal (Exp. PF_B2 in Figure 11). It is noteworthy that the DA-based estimation of forecast parameters may be affected by the equifinality issue (Thiboult et al., 2016),

when accounting for parameter uncertainty. In this undesired case, since single-member simulations are equally likely, the DA-based estimation of forecast parameters may provide suboptimal estimates. The PF-based analysis is mainly affected by the equifinality issue, which undermines forecast accuracy owing to a misrepresentation of system hydrological responsiveness. The limitation of parameter perturbation is not an efficient approach to reliably prevent possible overdispersion of parameter values (Noh et al., 2011b).

The results of this study stress the critical importance of a comprehensive representation of system uncertainties to derive the most benefit from the DA-based estimation of forecast ICs. The predictive accuracy is differentially sensitive and affected by each source of model uncertainty, which is likely to have a differing impact depending mainly on the choice of DA technique and modeling scheme. This is the case for threshold-based processes involved in the model dynamics, which can significantly undermine the propagation of meteorological uncertainty to the forecast initial states, leading to overconfidence in forecast ICs. The perturbation of model states can be an effective approach to jointly account for different sources of uncertainty affecting model predictions. However, it is of key importance to perform preliminary analyses in order to identify the model states most correlated with the assimilated observation, whose perturbation can allow for a more effective DA-based improvement of predictive accuracy. Conversely, the combined effect of the increase in the state variances and their slight correlation with the observed quantity can lead to a suboptimal estimation of their initial values. The uncertainty in model parameters is a more critical issue, as their suboptimal estimation can significantly undermine predictive accuracy due to a misleading representation of the hydrological response of the watershed throughout the forecast horizon. While the updating of forecast parameters can be challenging especially for conceptual models, it is likely to be more straightforward in physically based models, where parameters are generally more closely correlated with the assimilated variables.

6. Conclusions

This study addresses the sensitivity of DA-based estimation of streamflow forecast ICs to several sources of uncertainty and to the update of different states and parameters of the GR5J conceptual rainfall–runoff model, in terms of efficiency as well as temporal persistence. Both the EnKF and the PF schemes reveal straightforward applicability and effective usefulness to improve predictive accuracy by the assimilation of observed discharges at the forecast time.

When dealing with the assimilation of streamflow observations into a conceptual reservoir-based hydrological model, the main interest should be focused on improving the estimate of the initial level of the routing store in order to derive the most benefit from the DA-based estimation of forecast ICs (Rakovec et al., 2012, 2015).

When accounting only for meteorological uncertainty, EnKF-based forecasts outperform PF-based ones in terms of predictive accuracy. Indeed, since the latter technique is more sensitive to ensemble spread, during no-rain periods, the PF-based estimate of forecast ICs can result in less accurate streamflow forecasts.

A comprehensive representation of both meteorological and state uncertainties allows for a more efficient improvement of predictive skill. Indeed, while the accuracy of the PF-based estimation of forecast ICs is greatly improved, with a longer-lasting updating effect, the efficiency of the EnKF is enhanced only in the forecast short term.

Results show that parameter uncertainty can undermine predictive accuracy, since the DA-based estimate of forecast parameters is likely to significantly modify hydrological responsiveness through the update of production as well as routing store levels. In order to further assess the usefulness of the DA estimate of forecast parameters, an extensive analysis should be undertaken to compare the performance of the EnKF state augmentation with other approaches, such as the dual estimation proposed by Moradkhani, Hsu, et al. (2005). Furthermore, the efficiency of the kernel smoothing of parameters should be investigated to prevent possible over and underdispersion (Xie & Zhang, 2013).

When using the conceptual rainfall-runoff GR5J model, the suitability of the EnKF and PF schemes for streamflow forecasting mainly depends on the forecast horizon and the ultimate objectives of predictions. Indeed, while EnKF-based forecast ICs succeed in more efficiently improving predictive accuracy in the

short term, the PF-based estimation of forecast ICs guarantees a longer-lasting updating effect over the forecast horizon. Even though a PF-based forecasting system can be computationally more expensive owing to the large number of particles required (Weerts & El Serafy, 2006), this burden can be easily and effectively managed by parallelization (Noh et al., 2013). In this lumped application, the EnKF and PF schemes do not reveal a significant difference in computational time (about 10 min to perform daily DA-based simulations over the 6-year analysis period). In this regard, it will be useful to test the robustness and effectiveness of this DA-based forecasting system at the hourly time step, in order to assess its potentialities for short-term operational real-time forecasting.

This study is intended to provide useful recommendations to be referred to when dealing with DA-based forecasting systems relying on conceptual hydrological models.

The sensitivity of a forecasting system needs to be specifically investigated, as it largely depends on the modeling scheme and its representation of hydrological processes. When dealing with physically based hydrological models, the potential of DA-based estimates of forecast parameters needs to be assessed. Indeed, a higher correlation of the observed quantities with the model parameters describing physical processes is supposed to mitigate the equifinality issue. It is noteworthy that the benefit in updating specific state variables also depends on the assimilated observations. When assimilating observations of the surface soil moisture, the DA-based estimation of the forecast initial states of the production module can be a more suited approach to improve the predictive skill, rather than those of the routing module.

The spatial analysis of the performance of the DA-based forecasting system at the 232 analyzed watersheds revealed that the predictive accuracy does not depend on the local catchment conditions. Indeed, no apparent relationship can be identified between reliability of the DA-based forecasts and both topographic (e.g., surface, slope, altitude) and hydroclimatic (e.g., hydrological regime) parameters. However, it is noteworthy that the great part of the French catchments included in the analyzed dataset is characterized by pluvial river flow regimes. Therefore, further assessments are needed to investigate specific case studies that are not included in the analyzed sample, namely watersheds affected by severe drought periods, snowmelt dynamics or groundwater upwelling. However, it is noteworthy that the most ruling factor affecting the DA-based forecasting system is still the quality of the observations to be assimilated.

The proposed testing procedure can be generally useful to design a new forecasting system by properly identifying the most suitable DA method and its optimal configuration, as well as to diagnose possible deficiencies in existing forecasting systems.

Appendix A

Table A1
A Nonexhaustive List of the Studies Reported in the Literature Review

Reference	DA technique	Main system settings	Hydrological model	Key results
Thiboult et al. (2016)	EnKF	Different sources of uncertainty and ensemble sizes	20 conceptual lumped models (20 basins)	EnKF-based updating effect fades quickly
Maxwell et al. (2018)	EnKF	Uncertainty of model states, 100 members	Lumped conceptual model (1 basin)	Need for combined mass and flux constraints
DeChant and Moradkhani (2011)	PF	Uncertainty in meteorological inputs, 500 members	SAC-SMA model (1 basin)	Importance of the representation of IC uncertainty
Weerts and El Serafy (2006)	EnKF vs PF	Uncertainty in meteorological inputs, different ensemble sizes	HBV-96 model (16 sub-basins)	PF outperforms EnKF for a larger number of particles; lower sensitivity of EnKF to system uncertainties
Noh et al. (2013)	EnKF vs PF	Uncertainty in model states	WEP model (1 basin)	Higher and longer-lasting accuracy of PF-based forecasts

Table A1
Continued

Reference	DA technique	Main system settings	Hydrological model	Key results
Moradkhani, Sorooshian, et al. (2005)	EnKF (dual estimation)	Uncertainty in model inputs and parameters, 50 members	HyMOD (1 basin)	Kernel smoothing to prevent over and underdispersion of parameter values
Xie and Zhang (2013)	EnKF (dual estimation)	Uncertainty in model parameters and precipitation	SWAT model (20 sub-basins)	Potential of an EnKF-based partitioned forecast-update scheme
Moradkhani, Hsu, et al. (2005)	PF (dual estimation)	Uncertainty in model parameters and inputs, 1,000 particles	HyMOD model (1 basin)	Accurate state–parameter uncertainty estimation

Note. Each research study is characterized by the analyzed data assimilation (DA) technique/s, the system settings, the hydrological model used, and the key results.

Data Availability Statement

Meteorological data can be freely provided by Météo France, upon request, (https://publitheque.meteo.f) for research and nonprofit purposes. Streamflow data are publicly available on the Banque Hydro website http://hydro.eaufrance.fr/. An R package named *airGRdatassim* (Piazzi & Delaigue, 2021) is available on GitLab (https://gitlab.irstea.fr/HYCAR-Hydro/airgrdatassim). *airGRdatassim* is a package based on the airGR hydrological modeling package and it provides the tools to perform the assimilation of the observed discharges via Ensemble Kalman filter or Particle filter, according to the methodology presented in this paper.

Acknowledgments
The authors would like to thank Météo-France and SCHAPI for providing climate and streamflow data, respectively. This work was supported by the French Ministry of Ecology (DPGR/SNRH/SCHAPI, grant 2102615443), by the RenovRisk-Transfert project (OSU-Réunion, FEDER), by the SPAWET project (Centre national d'études spatiales, programme TOSCA) and by the PICS project (Agence nationale de la recherche, grant ANR – 17 – CE03 – 0011). The authors thank Wade Crow, Albrecht Weerts and an anonymous reviewer for their constructive comments, which helped to improve the quality of the article.

References

Alfieri, L., Burek, P., Dutra, E., Krzeminski, B., Muraro, D., Thielen, J., & Pappenberger, F. (2013). GloFAS-global ensemble streamflow forecasting and flood early warning. *Hydrology and Earth System Sciences*, *17*(3), 1161. https://doi.org/10.5194/hess-17-1161-2013

Alfieri, L., Pappenberger, F., Wetterhall, F., Haiden, T., Richardson, D., & Salamon, P. (2014). Evaluation of ensemble streamflow predictions in Europe. *Journal of Hydrology*, *517*, 913–922. https://doi.org/10.1016/j.jhydrol.2014.06.035

Alfieri, L., Salamon, P., Pappenberger, F., Wetterhall, F., & Thielen, J. (2012). Operational early warning systems for water-related hazards in Europe. *Environmental Science and Policy*, *21*, 35–49. https://doi.org/10.1016/j.envsci.2012.01.008

Alfieri, L., & Thielen, J. (2015). A European precipitation index for extreme rain-storm and flash flood early warning. *Meteorological Applications*, *22*(1), 3–13. https://doi.org/10.1002/met.1328

Anctil, F., & Ramos, M. H. (2018). Verification metrics for hydrological ensemble forecasts. In Q. Duan, F. Pappenberger, J. Thielen, A. Wood, H. Cloke, & J. Schaake (Eds.), *Handbook of hydrometeorological ensemble forecasting*. Berlin, Heidelberg: Springer. https://doi.org/10.1007/978-3-642-40457-3_3-1

Arulampalam, M. S., Maskell, S., Gordon, N., & Clapp, T. (2002). A tutorial on particle filters for online nonlinear/non-Gaussian Bayesian tracking. *IEEE Transactions on Signal Processing*, *50*(2), 174–188. https://doi.org/10.1109/78.978374

Berthet, L. (2010). *Flood forecasting at the hourly time step: Toward a better assimilation of flow information in a hydrological model (in French)* (PhD thesis). Cemagref (Antony), AgroParisTech (Paris), Paris, p. 603. Retrieved from https://webgr.inrae.fr/wp-content/uploads/2012/07/2010-BERTHET-THESE.pdf

Blöschl, G., Bierkens, M. F., Chambel, A., Cudennec, C., Destouni, G., Fiori, A., et al. (2019). Twenty-three unsolved problems in hydrology (UPH)–a community perspective. *Hydrological Sciences Journal*, *64*(10), 1141–1158. https://doi.org/10.1080/02626667.2019.1620507

Blöschl, G., Hall, J., Parajka, J., Perdigão, R. A., Merz, B., Arheimer, B., et al. (2017). Changing climate shifts timing of European floods. *Science*, *357*(6351), 588–590. https://doi.org/10.1126/science.aan2506

Blöschl, G., Reszler, C., & Komma, J. (2008). A spatially distributed flash flood forecasting model. *Environmental Modelling and Software*, *23*(4), 464–478. https://doi.org/10.1016/j.envsoft.2007.06.010

Boucher, M. A., & Ramos, M. H. (2018). Ensemble streamflow forecasts for hydropower systems. In Q. Duan, F. Pappenberger, J. Thielen, A. Wood, H. Cloke, & J. Schaake (Eds.), *Handbook of hydrometeorological ensemble forecasting*. Berlin, Heidelberg: Springer. https://doi.org/10.1007/978-3-642-40457-3_54-1

Boyle, D. P., Gupta, H. V., Sorooshian, S., Koren, V., Zhang, Z., & Smith, M. (2001). Toward improved streamflow forecasts: Value of semi-distributed modeling. *Water Resources Research*, *37*(11), 2749–2759. https://doi.org/10.1029/2000WR000207

Brown, J. D., Wu, L., He, M., Regonda, S., Lee, H., & Seo, D. J. (2014). Verification of temperature, precipitation, and streamflow forecasts from the NOAA/NWS Hydrologic Ensemble Forecast Service (HEFS): 1. Experimental design and forcing verification. *Journal of Hydrology*, *519*, 2869–2889. https://doi.org/10.1016/j.jhydrol.2014.05.028

Burnash, R. J. C., Ferral, R. L., & McGuire, R. A. (1973). *A generalized streamflow simulation system: Conceptual modeling for digital computers*, Jt. Fed. and State River Forecast Cent., U.S. Natl. Weather Serv. And Calif. Dep. of Water Resour., Sacramento.

Butts, M. B., Payne, J. T., Kristensen, M., & Madsen, H. (2004). An evaluation of the impact of model structure on hydrological modelling uncertainty for streamflow simulation. *Journal of Hydrology*, *298*(1-4), 242–266. https://doi.org/10.1016/j.jhydrol.2004.03.042

Chen, H., Yang, D., Hong, Y., Gourley, J. J., & Zhang, Y. (2013). Hydrological data assimilation with the Ensemble Square-Root-Filter: Use of streamflow observations to update model states for real-time flash flood forecasting. *Advances in Water Resources*, *59*, 209–220. https://doi.org/10.1016/j.advwatres.2013.06.010

Clark, M. P., Rupp, D. E., Woods, R. A., Zheng, X., Ibbitt, R. P., Slater, A. G., et al. (2008). Hydrological data assimilation with the ensemble Kalman filter: Use of streamflow observations to update states in a distributed hydrological model. *Advances in Water Resources*, *31*(10), 1309–1324. https://doi.org/10.1016/j.advwatres.2008.06.005

Cloke, H. L., & Pappenberger, F. (2009). Ensemble flood forecasting: A review. *Journal of Hydrology*, *375*(3-4), 613–626. https://doi.org/10.1016/j.jhydrol.2009.06.005

Coron, L., Delaigue, O., Thirel, G., Perrin, C., & Michel, C. (2020). *airGR: Suite of GR hydrological models for precipitation-runoff modelling. R package version 1.4.3.65*. https://doi.org/10.15454/EX11NA. Retrieved from https://CRAN.R-project.org/package=airGR

Coron, L., Thirel, G., Delaigue, O., Perrin, C., & Andréassian, V. (2017). The suite of lumped GR hydrological models in an R package. *Environmental Modelling and Software*, *94*, 166–171. https://doi.org/10.1016/j.envsoft.2017.05.002

Cuo, L., Pagano, T. C., & Wang, Q. J. (2011). A review of quantitative precipitation forecasts and their use in short-to medium-range streamflow forecasting. *Journal of Hydrometeorology*, *12*(5), 713–728. https://doi.org/10.1175/2011JHM1347.1

DeChant, C. M., & Moradkhani, H. (2011). Improving the characterization of initial condition for ensemble streamflow prediction using data assimilation. *Hydrology and Earth System Sciences*, *15*, 3399–3410. https://doi.org/10.5194/hess-15-3399-2011

DeChant, C. M., & Moradkhani, H. (2014). Toward a reliable prediction of seasonal forecast uncertainty: Addressing model and initial condition uncertainty with ensemble data assimilation and sequential Bayesian combination. *Journal of Hydrology*, *519*, 2967–2977. https://doi.org/10.1016/j.jhydrol.2014.05.045

Delaigue, O., Génot, B., Lebecherel, L., Brigode, P., & Bourgin, P. Y. (2020). *Database of watershed-scale hydroclimatic observations in France*. Université Paris-Saclay, INRAE, HYCAR Research Unit, Hydrology group, Antony. Retrieved from https://webgr.inrae.fr/base-de-donnees

Douc, R., & Cappé, O. (2005). Comparison of resampling schemes for particle filtering. *Proceedings of the 4th International Symposium on Image and Signal Processing and Analysis*, *2005*, 64–69.IEEE. https://doi.org/10.1109/ISPA.2005.195385

Doucet, A. (1998). Chapter 3 - On sequential simulation-based methods for Bayesian filtering. In *A. Doucet, Monte Carlo methods for Bayesian estimation of hidden Markov models. Application to radiation signals*, Ph.D. Thesis, Univ. Paris-Sud, Orsay, 1997. Retrieved from https://www.stats.ox.ac.uk/~doucet/doucet_sequentialsimulationbasedfiltering1998.pdf

Dumedah, G., & Coulibaly, P. (2013). Evaluating forecasting performance for data assimilation methods: The ensemble Kalman filter, the particle filter, and the evolutionary-based assimilation. *Advances in Water Resources*, *60*, 47–63. https://doi.org/10.1016/j.advwatres.2013.07.007

Emerton, R. E., Stephens, E. M., Pappenberger, F., Pagano, T. C., Weerts, A. H., Wood, A. W., et al. (2016). Continental and global scale flood forecasting systems. *Wiley Interdisciplinary Reviews: Water*, *3*(3), 391–418. https://doi.org/10.1002/wat2.1137

Evensen, G. (1994). Sequential data assimilation with a nonlinear quasi-geostrophic model using Monte Carlo methods to forecast error statistics. *Journal of Geophysical Research: Oceans*, *99*(C5), 10143–10162. https://doi.org/10.1029/94JC00572

Evensen, G. (2003). The ensemble Kalman filter: Theoretical formulation and practical implementation. *Ocean Dynamics*, *53*, 343–367. https://doi.org/10.1007/s10236-003-0036-9

Ficchì, A., Perrin, C., & Andréassian, V. (2016). Impact of temporal resolution of inputs on hydrological model performance: An analysis based on 2400 flood events. *Journal of Hydrology*, *538*, 454–470. https://doi.org/10.1016/j.jhydrol.2016.04.016

Franssen, H. J., & Kinzelbach, W. (2008). Real-time groundwater flow modeling with the ensemble Kalman filter: Joint estimation of states and parameters and the filter inbreeding problem. *Water Resources Research*, *44*(9), W09408. https://doi.org/10.1029/2007WR006505

Gordon, N. J., Salmond, D. J., & Smith, A. F. (1993). *Novel approach to nonlinear/non-Gaussian Bayesian state estimation*. In IEE Proceedings F (Radar and Signal Processing). (Vol. 140, No. 2, pp. 107–113). IET Digital Library. https://doi.org/10.1049/ip-f-2.1993.0015

Guingla, P., Antonio, D., De Keyser, R., De Lannoy, G., Giustarini, L., Matgen, P., & Pauwels, V. (2012). The importance of parameter resampling for soil moisture data assimilation into hydrologic models using the particle filter. *Hydrology and Earth System Sciences*, *16*(2), 375–390. https://doi.org/10.5194/hess-16-375-2012

Gupta, H. V., Kling, H., Yilmaz, K. K., & Martinez, G. F. (2009). Decomposition of the mean squared error and NSE performance criteria: Implications for improving hydrological modelling. *Journal of Hydrology*, *377*(1-2), 80–91. https://doi.org/10.1016/j.jhydrol.2009.08.003

Hao, Z., Singh, V. P., & Xia, Y. (2018). Seasonal drought prediction: advances, challenges, and future prospects. *Reviews of Geophysics*, *56*(1), 108–141. https://doi.org/10.1002/2016RG000549

Hapuarachchi, H. A. P., Wang, Q. J., & Pagano, T. C. (2011). A review of advances in flash flood forecasting. *Hydrological Processes*, *25*(18), 2771–2784. https://doi.org/10.1002/hyp.8040

Harrigan, S., Prudhomme, C., Parry, S., Smith, K., & Tanguy, M. (2018). Benchmarking ensemble streamflow prediction skill in the UK. *Hydrology and Earth System Sciences*, *22*(3), 2023–2039. https://doi.org/10.5194/hess-22-2023-2018

Hersbach, H. (2000). Decomposition of the continuous ranked probability score for ensemble prediction systems. *Weather and Forecasting*, *15*(5), 559–570. https://doi.org/10.1175/1520-0434(2000)015<0559:DOTCRP>2.0.CO;2

Julier, S., Uhlmann, J., & Durrant-Whyte, H. (1995). A new approach for filtering nonlinear systems. *In Proceedings of 1995 American Control Conference*. (pp. 1628–1632). Seattle, WA: IEEE. https://ieeexplore.ieee.org/abstract/document/529783

Kalman, R. E. (1960). A new approach to linear filtering and prediction problems. *Journal of basic Engineering*, *82*(1), 35–45. https://doi.org/10.1115/1.3662552

Kitagawa, G. (1996). Monte Carlo filter and smoother for non-Gaussian nonlinear state space models. *Journal of Computational and Graphical Statistics*, *5*(1), 1–25. https://doi.org/10.1080/10618600.1996.10474692

Leisenring, M., & Moradkhani, H. (2011). Snow water equivalent prediction using Bayesian data assimilation methods. *Stochastic Environmental Research and Risk Assessment*, *25*(2), 253–270. https://doi.org/10.1007/s00477-010-0445-5

Leleu, I., Tonnelier, I., Puechberty, R., Gouin, P., Viquendi, I., Cobos, L., et al. (2014). Re-founding the national information system designed to manage and give access to hydrometric data. *La Houille Blanche*, *1*, 25–32. https://doi.org/10.1051/lhb/2014004

Le Moine, N. (2008). *The catchment seen from underground: A way to improve the performance and realism of rainfall-runoff models? (In French)* (PhD thesis). Université Pierre et Marie Curie (Paris), Cemagref (Antony), p. 324. Retrieved from https://webgr.inrae.fr/wp-content/uploads/2012/07/2008-LE_MOINE-THESE.pdf

Li, H., Luo, L., Wood, E. F., & Schaake, J. (2009). The role of initial conditions and forcing uncertainties in seasonal hydrologic forecasting. *Journal of Geophysical Research: Atmosphere*, *114*, D04114. https://doi.org/10.1029/2008JD010969

Lindström, G., Johannson, B., Persson, M., Gardelin, M., & Bergström, S. (1997). Development and test of the distributed HBV-96 hydrological model. *Journal of Hydrology*, *201*, 272–288. https://doi.org/10.1016/S0022-1694(97)00041-3

Liu, Y., Weerts, A., Clark, M., Hendricks Franssen, H. J., Kumar, S., Moradkhani, H., et al. (2012). Advancing data assimilation in operational hydrologic forecasting: Progresses, challenges, and emerging opportunities. *Hydrology and Earth System Sciences*, *16*, 3863–3887. https://doi.org/10.5194/hess-16-3863-2012

Maxwell, D. H., Jackson, B. M., & McGregor, J. (2018). Constraining the ensemble Kalman filter for improved streamflow forecasting. *Journal of Hydrology*, *560*, 127–140. https://doi.org/10.1016/j.jhydrol.2018.03.015

McMillan, H. K., Hreinsson, E. Ö., Clark, M. P., Singh, S. K., Zammit, C., & Uddstrom, M. J. (2013). Operational hydrological data assimilation with the recursive ensemble Kalman filter. *Hydrology and Earth System Sciences*, *17*(1), 21–38. https://doi.org/10.5194/hess-17-21-2013

Miller, R. N., Ghil, M., & Gauthiez, F. (1994). Advanced data assimilation in strongly nonlinear dynamical systems. *Journal of the Atmospheric Sciences*, *51*(8), 1037–1056. https://doi.org/10.1175/1520-0469(1994)051<1037:ADAISN>2.0.CO;2

Montzka, C., Moradkhani, H., Weihermüller, L., Franssen, H. J. H., Canty, M., & Vereecken, H. (2011). Hydraulic parameter estimation by remotely-sensed top soil moisture observations with the particle filter. *Journal of Hydrology*, *399*(3-4), 410–421. https://doi.org/10.1016/j.jhydrol.2011.01.020

Moradkhani, H., Hsu, K. L., Gupta, H., & Sorooshian, S. (2005). Uncertainty assessment of hydrologic model states and parameters: Sequential data assimilation using the particle filter. *Water Resources Research*, *41*(5), W05012. https://doi.org/10.1029/2004WR003604

Moradkhani, H., Sorooshian, S., Gupta, H. V., & Houser, P. R. (2005). Dual state–parameter estimation of hydrological models using ensemble Kalman filter. *Advances in Water Resources*, *28*(2), 135–147. https://doi.org/10.1016/j.advwatres.2004.09.002

NCAR - Research Applications Laboratory. (2015). *Verification: Weather forecast verification utilities. R package version 1.42*. https://CRAN.R-project.org/package=verification

Noh, S. J., Rakovec, O., Weerts, A. H., & Tachikawa, Y. (2014). On noise specification in data assimilation schemes for improved flood forecasting using distributed hydrological models. *Journal of Hydrology*, *519*, 2707–2721. https://doi.org/10.1016/j.jhydrol.2014.07.049

Noh, S. J., Tachikawa, Y., Shiiba, M., & Kim, S. (2011a). Applying sequential Monte Carlo methods into a distributed hydrologic model: lagged particle filtering approach with regularization. *Hydrology and Earth System Sciences*, *15*, 3237–3251. https://doi.org/10.5194/hess-15-3237-2011

Noh, S. J., Tachikawa, Y., Shiiba, M., & Kim, S. (2011b). Dual state-parameter updating scheme on a conceptual hydrologic model using sequential Monte Carlo filters. *Annual Journal of Hydraulic Engineering, JSCE*, *55*, 1–6. https://doi.org/10.2208/jscejhe.67.I_1

Noh, S. J., Tachikawa, Y., Shiiba, M., & Kim, S. (2013). Sequential data assimilation for streamflow forecasting using a distributed hydrologic model: particle filtering and ensemble Kalman filtering. *Floods: From Risk to Opportunity*, *357*, 341–349. Retrieved from https://iahs.info/uploads/dms/15673.44-341-349-357-3-10_Noh.pdf

Noh, S. J., Weerts, A. H., Rakovec, O., Lee, H., & Seo, D. J. (2018). Assimilation of Streamflow Observations. In Q. Duan, F. Pappenberger, J. Thielen, A. Wood, H. Cloke, & J. Schaake (Eds.), *Handbook of hydrometeorological ensemble forecasting*. Berlin, Heidelberg: Springer. https://doi.org/10.1007/978-3-642-40457-3_33-2

Oudin, L., Hervieu, F., Michel, C., Perrin, C., Andréassian, V., Anctil, F., & Loumagne, C. (2005). Which potential evapotranspiration input for a lumped rainfall–runoff model? Part 2—Towards a simple and efficient potential evapotranspiration model for rainfall–runoff modelling. *Journal of Hydrology*, *303*(1-4), 290–306. https://doi.org/10.1016/j.jhydrol.2004.08.026

Pasetto, D., Camporese, M., & Putti, M. (2012). Ensemble Kalman filter versus particle filter for a physically-based coupled surface–subsurface model. *Advances in Water Resources*, *47*, 1–13. https://doi.org/10.1016/j.advwatres.2012.06.009

Pfahl, S., O'Gorman, P. A., & Fischer, E. M. (2017). Understanding the regional pattern of projected future changes in extreme precipitation. *Nature Climate Change*, *7*(6), 423. https://doi.org/10.1038/nclimate3287

Piazzi, G., & Delaigue, O. (2020). *airGRdatassim: Ensemble-Based Data Assimilation in GR Hydrological Models*. R package version 0.1.3. https://doi.org/10.15454/WEYYVZ

Pushpalatha, R., Perrin, C., Le Moine, N., Mathevet, T., & Andréassian, V. (2011). A downward structural sensitivity analysis of hydrological models to improve low-flow simulation. *Journal of Hydrology*, *411*(1-2), 66–76. https://doi.org/10.1016/j.jhydrol.2011.09.034

Rakovec, O., Weerts, A. H., Hazenberg, P., Torfs, P. J. J. F., & Uijlenhoet, R. (2012). State updating of a distributed hydrological model with Ensemble Kalman Filtering: effects of updating frequency and observation network density on forecast accuracy. *Hydrology and Earth System Sciences*, *16*(9), 3435–3449. https://doi.org/10.5194/hess-16-3435-2012

Rakovec, O., Weerts, A. H., Sumihar, J., & Uijlenhoet, R. (2015). Operational aspects of asynchronous filtering for flood forecasting. *Hydrology and Earth System Sciences*, *19*, 2911–2924. https://doi.org/10.5194/hess-19-2911-2015

Reed, S., Koren, V., Smith, M., Zhang, Z., Moreda, F., Seo, D. J., & DMIP Participants. (2004). Overall distributed model intercomparison project results. *Journal of Hydrology*, *298*(1-4), 27–60. https://doi.org/10.1016/j.jhydrol.2004.03.031

Reichle, R. H., McLaughlin, D. B., & Entekhabi, D. (2002). Hydrologic data assimilation with the ensemble Kalman filter. *Monthly Weather Review*, *130*(1), 103–114. https://doi.org/10.1175/1520-0493(2002)130<0103:HDAWTE>2.0.CO;2

Ricci, S., Piacentini, A., Thual, O., Pape, E. L., & Jonville, G. (2011). Correction of upstream flow and hydraulic state with data assimilation in the context of flood forecasting. *Hydrology and Earth System Sciences*, *15*(11), 3555–3575. https://doi.org/10.5194/hess-15-3555-2011

Salamon, P., & Feyen, L. (2009). Assessing parameter, precipitation, and predictive uncertainty in a distributed hydrological model using sequential data assimilation with the particle filter. *Journal of Hydrology*, *376*(3-4), 428–442. https://doi.org/10.1016/j.jhydrol.2009.07.051

Samuel, J., Coulibaly, P., Dumedah, G., & Moradkhani, H. (2014). Assessing model state and forecasts variation in hydrologic data assimilation. *Journal of Hydrology*, *513*, 127–141. https://doi.org/10.1016/j.jhydrol.2014.03.048

Sauquet, E., Gottschalk, L., & Krasovskaia, I. (2008). Estimating mean monthly runoff at ungauged locations: An application to France. *Hydrology Research*, *39*(5-6), 403–423. https://doi.org/10.2166/nh.2008.331

Schaake, J., Franz, K., Bradley, A., & Buizza, R. (2006). The hydrologic ensemble prediction experiment (HEPEX). *Hydrology and Earth System Sciences Discussions*, *3*(5), 3321–3332. https://doi.org/10.5194/hessd-3-3321-2006

Schaake, J., Hamill, T. M., Buizza, R., & Clark, M. (2007). HEPEX: the hydrological ensemble prediction experiment. *Bulletin of the American Meteorological Society*, *88*(10), 1541–1548. https://doi.org/10.1175/BAMS-88-10-1541

Shukla, S., & Lettenmaier, D. P. (2011). Seasonal hydrologic prediction in the United States: understanding the role of initial hydrologic conditions and seasonal climate forecast skill. *Hydrology and Earth System Sciences*, *15*(11), 3529–3538. https://doi.org/10.5194/hess-15-3529-2011

Sing, T., Sander, O., Beerenwinkel, N., & Lengauer, T. (2005). ROCR: visualizing classifier performance in R. *Bioinformatics*, *21*(20), 3940–3941. Retrieved from http://rocr.bioinf.mpi-sb.mpg.de

Sun, L., Nistor, I., & Seidou, O. (2015). Streamflow data assimilation in SWAT model using Extended Kalman Filter. *Journal of Hydrology*, *531*, 671–684. https://doi.org/10.1016/j.jhydrol.2015.10.060

Sun, Y., Bao, W., Valk, K., Brauer, C. C., Sumihar, J., & Weerts, A. H. (2020). Improving forecast skill of lowland hydrological models using ensemble Kalman filter and unscented Kalman filter. *Water Resources Research*, *56*(8), e2020WR027468. https://doi.org/10.1029/2020wr027468

Szewrański, S., Chruściński, J., Kazak, J., Świąder, M., Tokarczyk-Dorociak, K., & Żmuda, R. (2018). Pluvial flood risk assessment tool (PFRA) for rainwater management and adaptation to climate change in newly urbanised areas. *Water*, *10*(4), 386. https://doi.org/10.3390/w10040386

Thiboult, A., Anctil, F., & Boucher, M. A. (2016). Accounting for three sources of uncertainty in ensemble hydrological forecasting. *Hydrology and Earth System Sciences*, *20*(5), 1809–1825. https://doi.org/10.5194/hess-20-1809-2016

Thielen, J., Bartholmes, J., Ramos, M. H., & Roo, A. D. (2009). The European flood alert system–part 1: concept and development. *Hydrology and Earth System Sciences*, *13*(2), 125–140. https://doi.org/10.5194/hess-13-125-2009

Thiemig, V., Bisselink, B., Pappenberger, F., & Thielen, J. (2015). A pan-African medium-range ensemble flood forecast system. *Hydrology and Earth System Sciences*, *19*, 3365–3385. https://doi.org/10.5194/hess-19-3365-2015

Thirel, G., Martin, E., Mahfouf, J. F., Massart, S., Ricci, S., & Habets, F. (2010). A past discharges assimilation system for ensemble streamflow forecasts over France–Part 1: Description and validation of the assimilation system. *Hydrology and Earth System Sciences*, *14*, 1623–1637. https://doi.org/10.5194/hess-14-1623-2010

Thirel, G., Rousset-Regimbeau, F., Martin, E., & Habets, F. (2008). On the impact of short-range meteorological forecasts for ensemble streamflow predictions. *Journal of Hydrometeorology*, *9*(6), 1301–1317. https://doi.org/10.1175/2008JHM959.1

Trambauer, P., Werner, M., Winsemius, H. C., Maskey, S., Dutra, E., & Uhlenbrook, S. (2015). Hydrological drought forecasting and skill assessment for the Limpopo River basin, southern Africa. *Hydrology and Earth System Sciences*, *19*(4), 1695–1711. https://doi.org/10.5194/hess-19-1695-2015

Vidal, J. P., Martin, E., Franchistéguy, L., Baillon, M., & Soubeyroux, J. M. (2010). A 50-year high-resolution atmospheric reanalysis over France with the Safran system. *International Journal of Climatology*, *30*(11), 1627–1644. https://doi.org/10.1002/joc.2003.10.1002/joc.2003

Vrugt, J. A., Gupta, H. V., Nualláin, B., & Bouten, W. (2006). Real-time data assimilation for operational ensemble streamflow forecasting. *Journal of Hydrometeorology*, *7*(3), 548–565. https://doi.org/10.1175/JHM504.1

Vrugt, J. A., & Robinson, B. A. (2007). Treatment of uncertainty using ensemble methods: Comparison of sequential data assimilation and Bayesian model averaging. *Water Resources Research*, *43*(1). W01411. https://doi.org/10.1029/2005WR004838

Wang, C. H., & Bai, Y. L. (2008). Algorithm for real time correction of stream flow concentration based on Kalman filter. *Journal of Hydrologic Engineering*, *13*(5), 290–296. https://doi.org/10.1061/(ASCE)1084-0699(2008)13:5(290)

Wang, D., Chen, Y., & Cai, X. (2009). State and parameter estimation of hydrologic models using the constrained ensemble Kalman filter. *Water Resources Research*, *45*(11), W11416. https://doi.org/10.1029/2008WR007401

Weerts, A. H., & El Serafy, G. Y. (2006). Particle filtering and ensemble Kalman filtering for state updating with hydrological conceptual rainfall-runoff models. *Water Resources Research*, *42*(9), W09403. https://doi.org/10.1029/2005WR004093

Werner, M., Schellekens, J., Gijsbers, P., van Dijk, M., van den Akker, O., & Heynert, K. (2013). The Delft-FEWS flow forecasting system. *Environmental Modelling and Software*, *40*, 65–77. https://doi.org/10.1016/j.envsoft.2012.07.010

Wood, A. W., Hopson, T., Newman, A., Brekke, L., Arnold, J., & Clark, M. (2016). Quantifying streamflow forecast skill elasticity to initial condition and climate prediction skill. *Journal of Hydrometeorology*, *17*(2), 651–668. https://doi.org/10.1175/JHM-D-14-0213.1

Xie, X., & Zhang, D. (2010). Data assimilation for distributed hydrological catchment modeling via ensemble Kalman filter. *Advances in Water Resources*, *33*(6), 678–690. https://doi.org/10.1016/j.advwatres.2010.03.012

Xie, X., & Zhang, D. (2013). A partitioned update scheme for state-parameter estimation of distributed hydrologic models based on the ensemble Kalman filter. *Water Resources Research*, *49*(11), 7350–7365. https://doi.org/10.1002/2012WR012853

Yan, H., & Moradkhani, H. (2016). Combined assimilation of streamflow and satellite soil moisture with the particle filter and geostatistical modeling. *Advances in Water Resources*, *94*, 364–378. https://doi.org/10.1016/j.advwatres.2016.06.002

Yan, H., Moradkhani, H., & Zarekarizi, M. (2017). A probabilistic drought forecasting framework: A combined dynamical and statistical approach. *Journal of Hydrology*, *548*, 291–304. https://doi.org/10.1016/j.jhydrol.2017.03.004

Yesilnacar, E. K. (2005). *The application of computational intelligence to landslide susceptibility mapping in Turkey*. PhD Thesis, University of Melbourne, Department, p. 200. Retrieved from http://cat.lib.unimelb.edu.au/record=b2995654~S6

Yossef, N. C., Winsemius, H., Weerts, A., van Beek, R., & Bierkens, M. F. (2013). Skill of a global seasonal streamflow forecasting system, relative roles of initial conditions and meteorological forcing. *Water Resources Research*, *49*(8), 4687–4699. https://doi.org/10.1002/wrcr.20350

Young, P. C. (2002). Advances in real-time flood forecasting. *Philosophical Transactions of the Royal Society of London - A*, *360*(1796), 1433–1450. https://doi.org/10.1098/rsta.2002.1008

Zappa, M., van Andel, S. J., & Cloke, H. L. (2018). Introduction to Ensemble Forecast Applications and Showcases. In Q. Duan, F. Pappenberger, J. Thielen, A. Wood, H. Cloke, & J. Schaake (Eds.), *Handbook of hydrometeorological ensemble forecasting*. Berlin, Heidelberg: Springer. https://doi.org/10.1007/978-3-642-40457-3_45-1